MONASH University

Aspects of Robustness in Laboratory and Field Biochemical Processes

Darren McMorran

Bachelor of Engineering (with Honours) in the field of Electrical and Computer Systems Engineering

A thesis submitted for the degree of Master of Engineering Science at
Monash University in 2018
Department of Mechanical & Aerospace Engineering

Copyright notice

Abstract

Accurate diagnostic tests are needed in order to combat infectious diseases. These tests often involve the use of biochemical processes, but in order for them to be widely available, wherein cost is strong consideration, they should be conducted in the field or in the laboratory with high degrees of robustness. The research and development efforts expended in this work covers some salient aspects of improving the robustness of systems in biochemical applications.

Within the laboratory, an alternative method of manipulating biochemical samples was developed for automated processes offers reliability and efficiency. Specifically, collision detection and spill avoidance systems combining inertial measurement devices and robotic arm technology that will result in more repeatable operations at lower cost, by reducing the risk of mishandling biochemical samples, has been developed. Through early collision detection and management, it has been shown that operators can resolve issues due to collisions in the working area in a timely manner. These improvements will reduce overall operating time in laboratories in a cost-effective manner.

A stabilisation method developed has been shown to provide new, reliable methods of transporting sensitive biochemical materials in rural areas through rough terrain. It is demonstrated to render immunity to uneven motion being able to affect processes such as dried blood spot collection during transport. Pre-processing of samples offers to reduce congestion in biochemical laboratories and improve efficiency of the system overall.
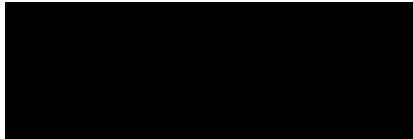
Finally, a motion and gust simulation platform developed using inertial moment sensing has been shown to provide information that will allow stabilisation methods to be refined and improved in order to be able to reduce the impact of motion experienced during transportation on samples under various real-world conditions. This will further reduce the likelihood of samples being damaged or spilled, and will also pave way for robust implementation of alternative transportation methods such as UAVs.

The research and development efforts expended in this project have been successful in advancing the effective use of technology to advance pertinent aspects of biochemical analysis in the laboratory and in the field.

Declaration

This thesis contains no material which has been accepted for the award of any other degree or diploma at any university or equivalent institution and that, to the best of my knowledge and belief, this thesis contains no material previously published or written by another person, except where due reference is made in the text of the thesis.

Signature: █████████████

Print Name: Darren McMorran.

Date: 05/01/18

Publications during enrolment

D. McMorran, D.C.K. Chung, J Li, M. Muradoglu, O.W. Liew, T.W. Ng,
Adapting a low-cost selective compliant articulated robotic arm for spillage avoidance.
Journal of Laboratory Automation. 21 (2016) 799-805.

M. Katariya, S.H. Huynh, D. McMorran, C.Y. Lau, M. Muradoglu, T.W. Ng,
Linear stepper actuation driving drop resonance and modifying hysteresis.
Langmuir. 32 (2016) 8550-8556.

D. McMorran, D.C.K. Chung, M. Toth, O.W. Liew, M. Muradoglu, T.W. Ng,
Stabilized dried blood spot collection.
Analytical Biochemistry. 506 (2016) 28-30.

Mayur Katariya, Chun Yat Lau, Darren McMorran, Alifa Afiah Ahmad Zahidi, Murat Muradoglu, Tuck Wah Ng, Gust simulator for small unmanned aerial vehicles, Aerospace Science and Technology. In Review.

Darren McMorran, Sewminda Kalana Samarasinghe, Murat Muradoglu, Dwayne Chung Kim Chung, Brett Williams, Oi Wah Liew, Tuck Wah Ng, Simulation training system for en-route intravenous initiation, Biosystems Engineering. Submitted 20/10/2017.

Acknowledgements

Table of Contents

1. Introduction

1.1 Background

One of the ongoing problems in the modern era is the frequency and significant impact of infectious disease outbreaks. With recent outbreaks of Ebola and Zika viruses, it is evident that outbreaks of infectious diseases have a significant impact on society either by direct damages of disease or the amount of time and resources required to mitigate further outbreak.

Analysis of data recorded in the Global Infectious Disease and Epidemiology Online Network shows that the total number of outbreaks and the amount of unique diseases have increased over time globally[1]. However, the severity of outbreaks has declined due to recent developments in infectious disease management including prevention, early detection, control and treatment.

Social tools have been explored to be fast detector of disease outbreaks[2]. Centrally located individuals in a social network are more susceptible to infection due to increased social ties. By monitoring these individuals for symptoms of disease, an outbreak can be detected significantly earlier than methods involving random individuals.

Once an outbreak is suspected, tools are required to identify the disease in order to plan treatment remedies. Standard procedure involves collecting blood samples of infected individuals and transporting them to biochemical laboratories for testing. While the developments in disease management mentioned aid to reduce outbreak severity, improvements to biochemical processes must also be developed in the field and laboratory. Figure 1 below shows the relationship between stages of infectious disease management and field and laboratory processes.
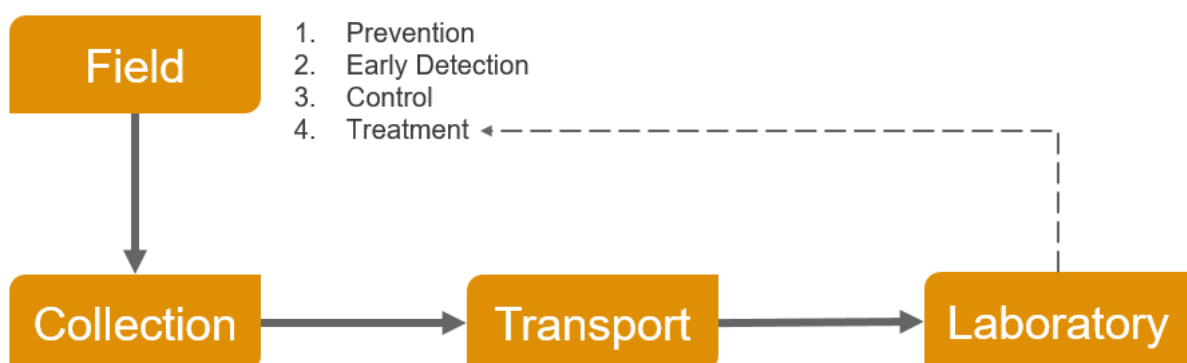

Figure 1 - Stages of infectious disease management in the laboratory and field

There have been recent developments in the use of robotics in the field to improve infectious disease management. The use of unmanned aerial vehicles (UAVs), or drones, to survey areas susceptible to disease outbreak as a means outbreak prevention is one of many

potential uses for robotics in the field[3]. Systems such as these are not currently widespread in use due to their limitations. Drone surveying is limited by environmental conditions such as wind, rain and clouds, as well as technological reasons such as battery failure.

Furthermore, recent improvements have been made to laboratories by implementing automation to several systems to improve efficiency and consistency. Current laboratory technologies are used to automate specimen transportation, inspection, accessioning and sorting[4]. However, these technologies have considerable flaws; some systems are restricted by limitations in the way they are used, while others are set back due to inconsistent and inflexible technology.

1.2 Objectives

This project aims to improve processes based on existing automation-assisted systems by developing robust solutions that increase reliability, efficiency and affordability. This includes using new technologies to reduce costs and implications, as well as researching new methods to overcome limitations of current systems.

The objectives of this research project are to:

- Explore innovative applications of new technology in laboratory automation processes and demonstrate improvements to robustness and affordability of existing methods

- Develop low-cost motion simulators capable of replicating the motion of transport and its effects on samples in a controlled laboratory environment

- Investigate methods to improve robustness of biochemical field processes including use of gust simulators to test reliability of unmanned aerial vehicles for surveillance and transportation applications.

1.3 Scope

This project encompasses several biochemical processes at different stages of infectious disease management in the laboratory and field. The flow chart shown in Figure 2 provides an illustration of the biochemical processes in scope of this study.
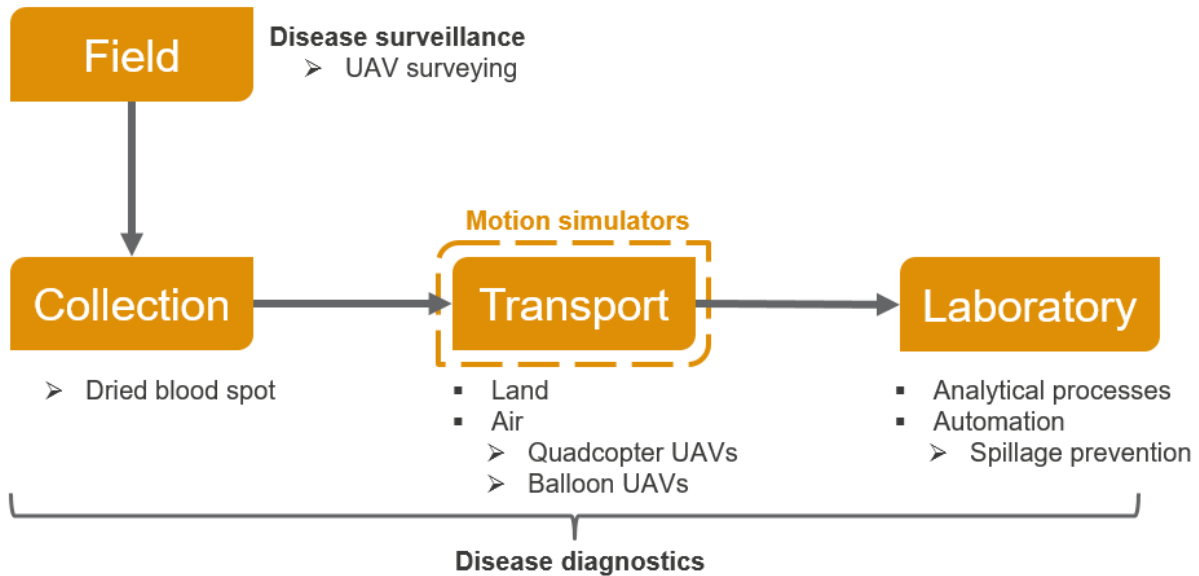
Figure 2 - Biochemical processes in the laboratory and field

The primary focus of this study explores improvements to robustness of disease diagnostic processes, an essential stage to identify and plan treatment of disease. This includes specimen collection methods such as dried blood spot, specimen transportation via land or air, and laboratory analytical processes and automation tools.

The scope extends beyond treatment processes through investigation of UAV surveying applications in the field for pre-emptive disease surveillance to prevent disease outbreak. Biochemical processes involved in early detection and control stages of infectious disease management are not explored in detail in this study.

2. Literature Review

The review furnished in this chapter is intended to provide an overview of the issues that this project seeks to address and the state-of-the art of the relevant current technologies. The research and development efforts that have been expended in this project to address some of these issues are described in the following chapters.

2.1 Integrated Disease Monitoring

2.1.1 Disease Surveillance

Disease surveillance is defined as an active, ongoing, formal, and systematic process aimed at early detection of a specific disease or agent in a population or early prediction of elevated risk of a population acquiring an infectious disease, with a prespecified action that would follow the detection of disease[5]. Surveillance systems are an essential stage of disease management that provide a foundation for control, treatment and prevention of infectious disease.

Early detection surveillance or post facto systems are used to monitor a target population and identify when a specific disease or agent has entered the population. Once identified, predefined actions aim to control the disease by preventing spread to other animals or herds. One example of such a system is the examination of culled cows for evidence of bovine flu identifiers.

Other surveillance systems aim to identify risk of disease outbreak pre-emptively, also known as risk surveillance systems. Environmental conditions and disease markers can be monitored to identify changes which increase risk of disease infecting a target population. By predicting when a disease is likely to outbreak, actions can be taken to prevent infection by reducing risk of outbreak. One such system has been used to monitor movements of macaques in areas under deforestation[3], a factor which is known to increase risk of infectious disease.

It is crucial that surveillance systems are able to identify elevated risks rapidly and accurately to ensure efficiency of appropriate actions in time critical situations. These factors have seen the introduction of various technologies in disease surveillance, including the use of Unmanned Aerial Vehicles (UAVs) to monitor disease management in the field.

2.1.2 Disease Diagnostics

Disease diagnostics performs a vital role in the management of infectious disease. A variety of diagnostic tools are used to identify infections or other pathogens present in patients in order to effectively plan and manage treatment. These tools collect information using various methods including imaging and biochemical technologies, pathological and psychological

investigations, and signs and symptoms elicited during history taking and clinical examinations[6].

Diagnostic tests are primarily used for patients who have identified signs or symptoms of a disease to monitor presence, grade and progression of infection. Due to the wide variety of tests available, it is important to have evidence of the accuracy of each test in order to utilise the best diagnostic method available. Diagnostic Test Accuracy (DTA) studies are used to compare accuracy of different tests, however the estimates of test accuracy frequently vary between studies[7].

There is continuous demand to develop diagnostic tests that are increasingly accurate in addition to improvements tin speed, cost, east of performance and patient safety[8]. These incentives have paved the way for automated systems which are able to use modern technology to perform diagnostics in laboratories to high precision and efficiency.

2.2 Laboratory Automation

2.2.1 History and Motivations

Automation in all its forms has played an integral role in society since the 19th century. Early automation systems were developed in manufacturing processes to perform tasks that were simple, repetitive and easy to replicate whilst improving efficiency. Continuous advancements in the fields of robotics and computer science in the last century have seen automation adapted to more complicated tasks such as those seen in biochemical laboratory processes.

There are a number of factors that have influenced the introduction and use of automation in the laboratory. Increases in infectious disease rates have led to high demand in laboratories to analyse samples and develop treatment solutions. Traditional laboratories face challenges to keep up with demand due to shortages in trained workers and associated costs. Furthermore, typical processes performed by workers in biochemical laboratories are often repetitive and require high concentration and precision. The nature of this work is prone to human error, often resulting in wasted samples and decreased efficiency. These challenges faced in traditional laboratories have been catalysts for the development of automated processes in biochemical laboratories.

The implementation of a laboratory automation system provides numerous benefits. Automated processes provide the improved efficiency necessary to manage escalating workloads at an affordable cost. Well-designed machines are able perform tasks with a high degree of accuracy, reducing delays experienced from mistakes in traditional methods. Automation also improves the wellbeing of workers by reducing health risks linked to biochemical handling and allows increased labour for more important and rewarding tasks.

Lastly, an automated laboratory system can provide overall process improvements by providing a simple workstation that is effective at managing inventory and requires lower training requirements for operators [9].

These benefits can be realised through automation of individual processes in laboratories from collection to analysis. Systems developed with partial automation of laboratory processes have demonstrated success in meeting most of the expectations of laboratory automation. However, these systems still require labour for overseeing and integrating separate automation systems. Completely automated systems, known as Total Laboratory Automation (TLA), have been able to overcome this issue by incorporating automation for all processes in the laboratory[4].

2.2.2 Cost Issues

Health systems across the globe are facing significant economic pressure to manage the rising costs from managing infectious disease, chronic illnesses and the aging population. Naturally, any system which is able to reduce working costs in this industry has been highly sought after to reduce economic strain.

While laboratory diagnostic tests only contribute a small portion of health care costs, the results influence of up to 70% of health care decision-making[10]. The accuracy of these results is vital to making correct decisions in turn reducing costs from errors and surplus testing.

Automation of diagnostic testing in the laboratory has the ability to process continually growing workloads at a sustainable cost. However, it is important to use cost-effective systems which are reliable enough to produce consistent results with low risk for errors. The importance of cost-effective solutions is especially critical in countries with low levels of health care. Countries with poor health systems are ill-equipped to manage the health care of individuals in areas where there are often higher rates of infectious disease.

2.2.3 Supporting Aspects in Laboratory Automation

2.2.3.1 Specimen Collection and Transportation

Specimen collection, transport, processing and storage are major sources of variation at the pre-analytical stage and quality management in these areas are the foundations of successful translational clinical research [11]. Blood is the most widely used liquid biopsy sample and is collected primarily via venepuncture for clinical laboratory testing. There is increasing evidence that analytical reliability and reproducibility is contingent on prompt separation of plasma and serum from blood cells as well as rapid storage at ultra-low temperatures [12]. The need to have the centrifugation instrumentation available at the point of sample collection to extract plasma and serum from the whole blood sample is understandably cumbersome. In addition, the logistics needed to provide refrigeration incurs significant costs in the process.

The dried blood spot (DBS) approach was arguably first reported in 1963 [13] as an alternative sample collection method for paediatric purposes. DBS typically comprises the deposition of a few drops of blood, obtained by a prick to the finger, onto filter papers in a card format. The samples are simply allowed to dry without any other processing. Notable advantages of the DBS method in terms of reduced sample volume, ease of sample collection, and analyte stability under ambient conditions has fuelled recognition of this technology as a viable alternative to plasma as the analytical matrix for storing and testing [14],[15],[16]. Various advances have been made in DBS sample processing. These included the incorporation of approaches such as polymerase chain reaction (PCR) [17], liquid chromatography [18], and Western blotting [19], sensitive detection methods such as mass spectrometry [10], as well as automation schemes to improve throughput [20]-[21]. During the collection phase, practitioners have to ensure that the sample is allowed to drop onto the centre of the guide circle on the DBS card and distribute evenly therein. The accuracy is adversely affected and/or invalidated if the sample is not collected properly and the spot size varies as a result of 1) co-joined spots where two spots are applied too closely and merge together, 2) smeared or splattered spots where blood is accidentally smeared before it is completely dried or splattered during spot application [22]. This can be difficult to accomplish if there is relative motion between the source of blood sample discharge, for example from a finger prick or a transfer capillary tube, and the DBS card. As a task that requires eye-hand coordination, such a situation will force the practitioner's nervous system to associate spatially separated signals and attempt to unify their perceptions for a coherent interpretation before issuing the appropriate motor command [23]. This is known to be mentally challenging and tiresome, leading to errors in the execution of tasks.

Transportation of collected samples within a testing facility is typically performed by human courier services which have inflexible pickup times and delays. These issues have influenced the development of various unmanned transportation systems. Pneumatic tube

systems have high efficiency for small volumes, however lack carrying capacity for high loads and may also result in damage from transportation[24]. Robotic couriers show potential for higher efficiency and lower costs than traditional courier systems, however may not be sufficiently reliable in practice[25]. Unmanned aerial vehicles have also shown promise for specimen transportation between collection and analysis facilities, especially in areas where infrastructure for manned courier services is undesirable.

2.2.3.2 Analytical Processes

The advantages of automation in laboratory analytical processes have been demonstrated with up to 80% of testing in clinical laboratories already impacted by automation[4]. Ongoing developments in laboratory automation utilise state of the art technology to perform more complicated processes with precision and efficiency. Such processes where automation is likely to grow in the future include microbiology, sample separation and cell-based assays.

Advanced computer software has been developed to aid in microbiology processes, utilising rapid sequencing of microbe DNA and RNA to identify individual organisms in an infection. Technologies such as Ion Torrent, Myseq, ionPGM, and PackBio are already demonstrating improved turnaround time and positive microbe identification in clinical settings[4]. Future technologies may incorporate software algorithms to compare DNA and RNA sequences with known pathogens for complete automation to reduce turnaround times. The Lawrence Livermore Microbial Detection Array is one type of similar process which is capable of identifying thousands of bacteria and viruses in a single test over 24 hours[26].

A variety of technologies have been developed to separate blood samples into serum or plasma for testing, a process which has historically limited the overall efficiency of testing facilities. The Axial Separation Module (ASM) provided significant reductions to separation time compared to conventional centrifugation [27]. However, separation technologies such as these have not been adopted in industry practice. As such, similar technologies are being investigated to develop an improved automated separation system.

Cell-based assays are another area which will be impacted by laboratory automation. Cell-based assays are used in diagnostics and to predict effectiveness of different treatment methods. One such application is the use of renal proximal tubule cells (RPTCs) to measure salt sensitivity of blood pressure[28], an issue with no convenient alternatives using traditional methods. It is anticipated that use of automation in this field will be developed as applications of cell-based assays in clinical laboratories continues to grow.

Various aspects of analytical processes in clinical laboratories have already seen improvements from automation technologies. These technologies have demonstrated reduced turnaround times and improved accuracy when processing samples for testing and analysis. However, some technologies are still being developed for analytical aspects which have not seen automation in practice due to complexity or insufficient volumes.

2.3 Relevant Engineering Aspects

2.3.1 Liquid Handling Stability

Considering that samples in the laboratory are almost always liquid, it is logical to consider the mechanics associated with its stability. An interesting remark made that "it is common everyday knowledge to each of us that any small container filled with liquid must be moved or carried very carefully to avoid spills" [29] continues to stir the interest of scientists to this day.

Why a container that holds liquid spills shows that it is a confluence of biomechanics, liquid sloshing engineering, and dynamical systems. While each of these subjects are well developed, the fact that they have different focuses of study does not allow one to penetrate into the posed question immediately. Namely, on one hand, a large body of the biomechanics and medical literature is dedicated to the study of human walking, including quantifying the motion of the body centre of mass [30], energy expenditure, and efficiency of process [31]; gait patterns related to gender, age, health, etc. [32][33]; motion of appendages (arms and legs) in natural positions [34]; and regularity of walking over long periods of time [35]. On the other hand, liquid sloshing studies are concerned with large liquid-filled structures such as rocket fuel tanks [29][36][37], which are subject to considerable accelerations and vibrations; forces and torques due to liquids experiencing various sloshing motions [38] and suppression of sloshing necessary for vehicle control [39][40]. However, in the walking with coffee problem the motions of the human body, while seemingly regular, are quite complex and are coupled to a coffee cup and liquid therein, which makes it difficult to unravel the precise reasons behind spilling.

It has been recently been shown [41] that spillage occurs either by accelerating too much for a given level (fluid statics) or through more complicated dynamical phenomena due to the particular range of sizes of common containers, which is dictated by the convenience of carrying them and the normal consumption. Namely, first the maximum acceleration occurring early on in the walking sets an initial sloshing amplitude. This interface deflection is then amplified by the back-and-forth and pitching excitations. Vertical excitation does not lead to resonance as it is a subharmonic excitation (Faraday phenomenon). The noise component of motion contains higher-frequency harmonics, which make the antisymmetric mode unstable, thus generating a swirl. Time to spill generally depends on whether walking is in a focused or unfocused regime and increases with decreasing maximum acceleration (walking speed). The difference between the focused and unfocused regimes suggests that walking with coffee is a control problem, since the number of steps to spill is different in these two regimes. As the data analysis shows, this is due to the difference in the level of a noise excitation, while the amplitude of a regular excitation does not change significantly, which is conceivably due to the natural constraints of the biomechanics of walking. However,

whether it is a feedback (closed loop) control system—i.e., when a human being "identifies" the resonant sloshing frequency and then performs a targeted suppression of the resonant mode—or an open loop control system—i.e., when a human being simply becomes more careful about carrying a cup regardless of the natural frequency of the fluid in it—may depend on an individual. However, it may be possible to control this with better precision using automation.

The prevention of spills in the laboratory has important implications. Chemicals in the liquid state are common in the laboratory. In many processes liquids are used as reactants or products, as well as coatings, solvents, fuels, additives, etc. In all of these capacities a liquid can evaporate to form a vapour. Once in the vapour phase chemicals are easily transferred, which increases environmental concerns because of their potential effects on sensitive human and ecological life.

Recent efforts [42] have been made to predict the evaporation rates and evaporation times for spills and constrained baths of chemical mixtures. Steady-state and time-varying predictions of evaporation rates can be made for six-component mixtures. A group-contribution method can also be used to estimate vapour-phase diffusion coefficients, which should make the method completely predictive. Yet the prevention of spillage offers better mitigation.

2.3.2 Robotic Arm Control

Robotics have played an important role in the automation industry since their development in the 20th century. One type of robot that has had a significant impact on this industry is the robotic arm. First developed in 1938[43], robotic arms now see pervasive use in automation applications due to their flexibility and efficiency.

Various types of robotic arms have been developed over time to suit different applications. Basic robotic arms such as Cartesian, Cylindrical and Polar Robots are limited to linear coordinate movements resulting in few degrees of freedom. More advanced robotic arms have up to six degrees of freedom, these include the Selective Compliance Assembly Robot Arm (SCARA) as well as Articulated and Parallel Robots. For some applications, it is necessary to have more degrees of freedom. Serpentine robot arms have been developed for use in robot-assisted surgery, the spine-based design allows operators to perform complex manoeuvres of up to 30 degrees of freedom. Another modern variation is the Anthropomorphic Robot Arm, which resembles a human arm with similar control to a human hand.

Whilst robotic arms have seen prevalent use in various fields ranging from manufacturing assembly lines to food handling systems, they have also played an important role within modern laboratories. Robotic arms provide many benefits to modern laboratories; including

efficiency, consistency and time and financial savings from reduced manual labour. Due to these benefits, robotic arms have been used to perform laboratory tasks varying from autonomous scientific discovery [44] to Total Laboratory Automation (TLA)[4]. Tasks such as these involve manoeuvring test samples around the laboratory using one or multiple robotic arms and require accurate and reliable positional control. For robust operation of robotic arms in a dynamic working space such as a laboratory, adaptability is essential to ensure machinery can adjust to changes made to its environment such as the addition or change in position of storage facilities.

One such method of improving robustness of robotic arms in laboratories involves implementing collision avoidance by traversing predetermined low-risk movement paths [45]. When the robot extends outside the safe zone, a series of positions are stored along the forward path to the destination. After completing tasks at the destination which may involve delivering a payload or manipulating a sample, heuristic algorithms are used to determine the safest return path based on stored positions. By choosing return paths based on stored positions, the robot can return to the safety zone with minimal risk of colliding with obstacles in the operating area. However, a system such as this may increase sturdiness by decreasing the chance of collisions, it is still not adaptable to new or frequent changes to the working space of the robotic arm.

2.3.3 Inertial Measurement

Inertial Measurement Units (IMUs) are devices that combine measurements from various accelerometers, gyroscopes and other sensors to determine angular position. Early IMU prototypes developed in the 1930s were large, expensive devices restricted to use in big projects such as aircraft navigation[46]. However, recent advances in microelectromechanical systems (MEMS) technology have resulted in a drastic reduction in the size and cost of IMUs. Modern IMUs are affordable for use in projects of all scales and are used in various applications ranging from navigation to robotics.

Different combinations of sensors are used in IMUs depending on the application. The simplest type of IMU incorporates a 3-axis accelerometer and 3 axis gyroscope which results in six degrees of freedom. This basic type of IMU is used in applications where more advanced devices may be unreliable due to disturbances in the surrounding magnetic field; however, the main drawback is the inaccuracy of data due to gyro drift and accelerometer limitations. To overcome these issues, more advanced IMUs incorporate a third sensor into the device: a magnetometer. This provides the IMU with measurements of the magnetic field in three different axes, resulting in 9 degrees of freedom. The additional sensor allows the IMU to operate accurately for long periods of time without experiencing issues from gyro drift by calibrating data from all three sensors.

Modern day reductions to the size and cost of IMUs have seen the devices used in a variety of applications. Within industrial fields, IMUs have been used in fastening tool tracking systems to improve quality control by reducing operator errors [47]-[48]. The tracking system enabled accurate positioning of tool tips, which ensures all bolts are fastened in a reliable and controlled manner. Similarly, IMUs have been integrated into sporting equipment to provide accurate feedback to an athlete's technique, such as the spin dynamics of a bowling ball[49]. There have also been works to combine IMUs with Global Position System (GPS) technology to improve reliability[50]. Measurements from the GPS and IMU are fused to create a method capable of detecting faults in the GPS navigation system.

IMUs have also found use in a wide range of robotics applications. They have been used in exoskeleton robots designed to help post-stroke upper limb rehabilitation by providing positional feedback of the stroke-affected arm [51]. StarlETH [52] is another robotics project incorporating use of IMUs in the design. The quadruped platform legged robot uses IMUs attached to each leg to measure the position of each of the robot's legs. Similarly, IMUs are expected to provide various benefits to robotic systems in biochemical laboratories. Measurements made by the sensors attached to arm linkages could provide helpful feedback which can be used to detection collisions and prevent tilting.

2.3.4 Motion Simulators

The immense growth in vehicle development during the 20th century has resulted in vehicular transport being an integral part of modern life. Manufacturing companies developed various types of mechanisms to simulate the motion experienced while driving. This trend has continued to the modern era, where motion simulators play an important role in developing safety and training systems. The application of motion simulators has extended to the commercial field, driving simulators for entertainment purposes are diverse and commonplace.

Early vehicle simulators developed by Honda in 1988 demonstrated the application to reproduce the experiencing of driving a motorcycle [53]. These devices were capable of simulation motion with 4 degrees of freedom: roll, pitch, yaw and handlebars steer. However, the absence of centripetal forces experienced while using the simulator presented a problem for users as the driving experience was noticeably different to real motorcycles.

More developed motion simulators have since been developed to provide a more accurate representation of vehicular motion. Some simulators have been built using large Stewart platforms which offer various advantages. The mechanism is able to simulate motion with 6 degrees of motion with the ability to control the centre of rotation of the platform. The latter value is a vital aspect in accurate vehicular motion simulation and has set the standard for future simulators.

Applications of motion simulators have commonly involved driving simulation for research or entertainment purposes. The continued significance of driving accidents has also seen various motion simulators developed to develop and test safety mechanisms in vehicles. The application of motion simulators can be extended to use in the biochemical laboratory, by using smaller platforms to simulate motion samples may experience during transportation.

2.3.5 Gyroscopic Stabilisation

A gyroscope is a device for measuring or maintaining orientation based on the principles of angular momentum. Since external torque is minimised by mounting the device on gimbals, its orientation remains nearly fixed, regardless of any motion of the platform on which it is mounted. With the advent of micro electromechanical systems (MEMS) technology, it was inevitable that micro-gyroscopes would begin to be developed to measure the angular rate of rotation. Due to the intensive research and development efforts in this field, micro-gyroscopes in the form of miniature chips have now become readily available at relatively low costs. The use of the sensing signals from these micro-gyroscopes in conjunction with actuation using inexpensive servo-motors, has resulted in the creation of compact and stabilised imaging systems that are now widely applied in unmanned aerial vehicle (UAV) photography [54].

Gyroscopic stabilisation has been adapted for use in various biochemical related applications in the laboratory [55]-[56]. The ability to keep biochemical samples stable prevents risks of sloshing and spillage due to external motion. Furthermore, gyroscopic stabilisation opens the way for method refinement to achieve accurate and valid DBS sample collection in situations where there is relative motion of the sample source with respect to the DBS card. It is important to note that this is applicable to situations of collecting samples from patients at the point of care or from animals. In the latter, the requirement for reduced number of animals and lower sampling volume fosters increased adoption of DBS for pharmacokinetic and toxicokinetic studies using animal models [57]. It is envisaged, for example, that with appropriate system modifications, the incorporation of the gyroscope stabilisation approach can improve blood collection from the lateral caudal vein of small rodents onto the DBS card where some movements are inevitable despite restraint by the animal handler or use of an animal restraining device.

2.3.6 Unmanned Aerial Vehicles

The potential benefits robotics can provide to processes in the field have increased significantly with the development of Unmanned Aerial Vehicles, or UAVs, and the abundance of applications they can perform. The main benefits of UAVs include the ability to monitor or provide transport in areas too dangerous or costly for manned aerial vehicles.

UAVs have been used in a variety of applications, ranging from use in agriculture to determine biophysical parameters of crops [58] to aiding disasters by providing hazard maps of dangerous areas [3].

One such application within the biochemical field involves using UAVs to transport test samples from rural clinics to central laboratories in Africa, where other methods would not suffice due to lack of road infrastructure [59]. Spread of HIV/AIDS saw increased demand on laboratory services, where it was economically infeasible to have the expensive equipment required for testing in each clinic. Use of UAVs to transport samples to testing laboratories proved to be advantageous to standard methods due to inadequate road structure.

Within the field of infectious disease management, UAVs have been used to survey areas susceptible to disease outbreak due to changes in land-use[3]. Deforestation is one form of change in land-use that has been recognised as a driving factor for infectious disease emergence. UAV surveying is able to provide accurate geospatial information necessary to estimate the risk of disease emergence and establish infectious disease prevention and control systems.

Typically, geospatial information is obtained from satellite-based remote sensing. This information is convenient as it uses existing technology, however the spatial resolution is considerably lower than information obtained via surveying. Furthermore, obtaining geospatial information via satellite at critical points in time is unfeasible, which is essential to map areas that have high rates of land-use change.

Information from UAV surveying is also limited by several factors. Environmental conditions such as wind, raid and cloud cover affect the usability data collected by UAVs. Moreover, flight time is limited by the UAV's battery, which in turn restricts the feasible surveying range. It is noteworthy that flight is inherently expensive energetically, and this is particularly so in when the size of the UAV is reduced. This is can be attributed to reductions in power density of the electromagnetic motors, as well as decreased transmission efficiencies due to the friction in gears and bearings. Flight modes such as hovering, which are often required in many phases during operation, is particularly challenging. This leads to the need to incorporate sensing devices properly[60]. It is hardly surprising then that considerable efforts have been made to model and analyse the flight stability of small UAVs [61]. From this, improved flight control strategies have been proposed [62].

Clearly, the versatility offered by UAVs portend applications in diverse fields. However, this is seldom explored. For instance, no reported efforts have been made to extend this technology to laboratory automation.

2.3.7 Gust Simulation

An alternative small UAV is based on blimps and balloons. Balloon UAVs are by nature low-flying, slow, long-endurance aircraft that provide a monitoring platform needed for long-term observation of an area. They are excellent instrument platforms, being steady and vibration-free. Unlike quadcopters, they can be filled with helium gas, which is lighter than air, and thus keeps them floating through air through the buoyant force. Balloon UAVs can hover over a site and observe environmental changes over long periods from various altitudes, providing high-resolution images at low cost [63]. They can also house compact multispectral imaging systems that monitor the blue, red, and near-infrared (NIR) spectral bands in order to provide more detailed information [64].

It remains desirable to physically test these flight models and flight control strategies using actual UAVs. In a wind-tunnel, the speed of airflow can be varied but typically only in a gradual fashion. Yet, the stability performance of small UAVs, particularly in the hovering mode, is affected more by gusts. A gust is a sudden, brief increase in the speed of the wind followed by a lull. One method to simulate gusts in a wind tunnel is to use arrays of oscillating vanes upstream of the wind tunnel test section [65]. This generates vertical (or lateral) velocity components according to the amplitude of the vane motion and the frequency of their operation. Alternative methods include having fixed aerofoils with oscillating vanes [66] and rotating cylinders with slots [67]. However, these appear better suited to simulating aircrafts operating at high flight speeds. Another approach of using banks of axial fans to test the response of small UAVs operating at relatively low airflow speeds has been reported [68].

When testing UAVs in a controlled environment, gust simulators have proven useful but difficult to control accurately without modifying the wind tunnel used.

3. Ascertaining Accuracy in Dried Blood Spot Collection & Testing

3.1 Introduction

During the collection phase of the dried blood spot method, practitioners have to ensure that there is no smearing of the blood sample on the filter paper, or readings from it will be invalid. This can be difficult to accomplish in the field if there is relative motion between the site of blood discharge on the finger and the filter paper. A gyroscope stabilisation method was developed and demonstrated to provide consistent and improved dried blood spot collection within a circular guide region notwithstanding the presence of rocking.

3.2 Gyroscopic Stabilisation Mechanisms

A low-cost gyroscope stabiliser was used to demonstrate the ability to perform accurate dried blood spot testing when in motion. The device consists of two motors that provide stabilisation in pitch and roll axes. Stabilisation in the yaw axis is unnecessary for dried blood spot testing, as small changes in yaw do not have a significant impact on the spread of the blood sample on the filter paper and there are no situations where a sample would be subject to large yaw fluctuations.

3.3 Rocking Motion Simulator

A rocking mechanism driven by a servomotor was devised for the experiment (see Figure 3) on which a gyroscope stabiliser was mounted (y). It comprised two platforms, one attached to the rocking mechanism directly (x), and another attached to the gimbal position of gyroscope stabiliser (z). The mechanism was controlled using an ATmega328P microcontroller, allowing specified rocking amplitude and frequency to be set and replicated in real-time.
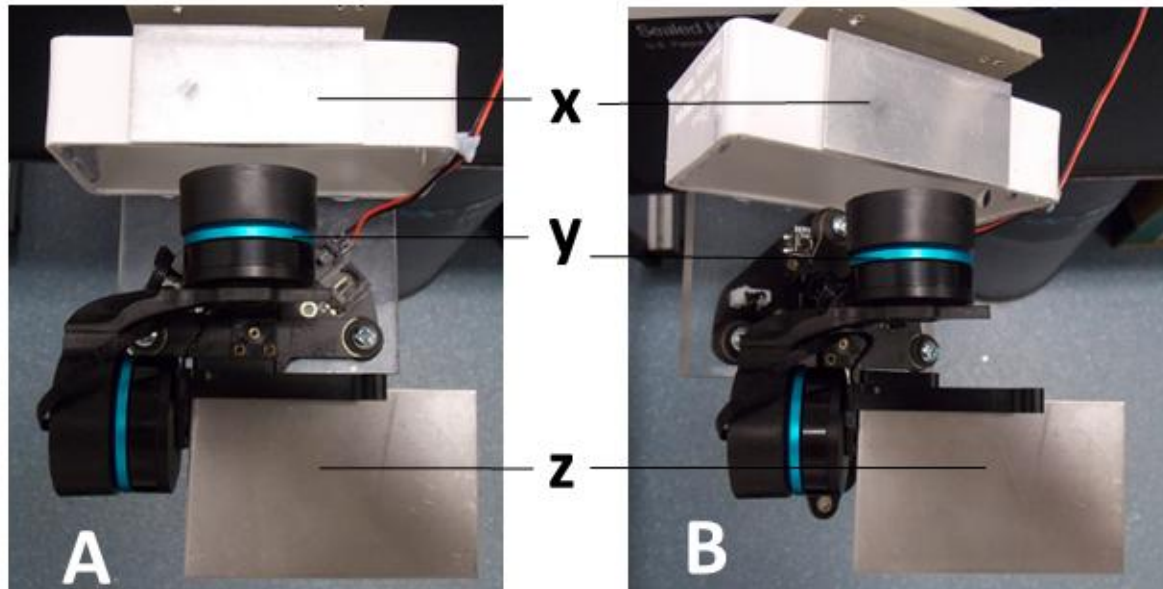
Figure 3 – Top view of rocking mechanism with gyroscope stabiliser at horizontal (A) and tilted (B) positions

3.4 Results and Discussion

The rocking motion simulator was designed to provide a basis for the analysis of dried blood spot testing under motion. The rocking motion comprised purely sinusoidal variation in the roll axis, which is a significantly simplified model of the motion samples would experience during vehicular motion.

During experiments, filter papers (Whatman) with a circle of 12 mm marked at their centres, were placed on the platforms x and z. While the mechanism was operating, a manual pipette (Eppendorf) was used to deposit 10 μL of blood sample at the centre of the marked circle from a constant height of 30 mm. The blood samples were drawn from the jugular vein located on the side of the sheep's neck. An 18-gauge needle was inserted into the vein and blood was drawn back into a syringe. The blood was then added to tubes with 0.5 mL of sodium citrate to prevent immediate clotting. After the blood samples dispensed on the filter paper were dried, they were placed on a flatbed scanner, which can be versatilely adapted to various uses [69][70], for image digitisation.
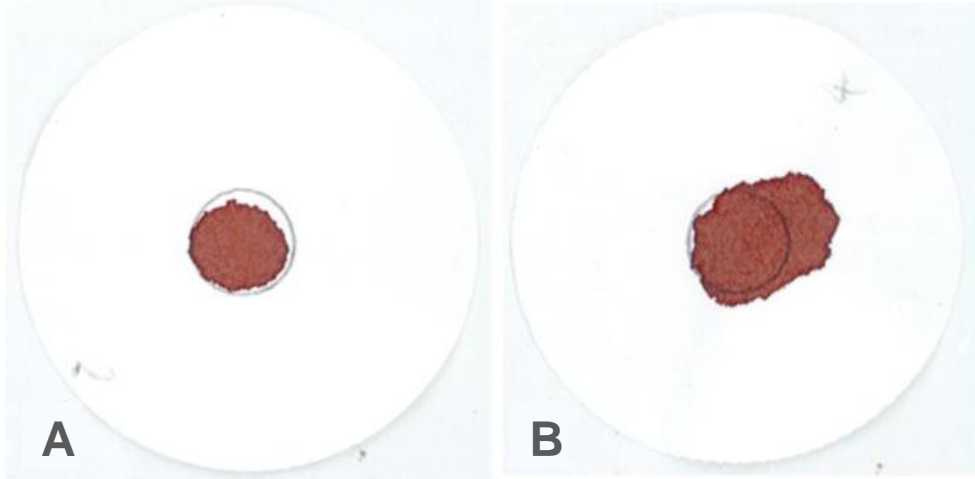
Figure 4 – Dried blood spot collection samples

With the gyroscope stabiliser, the platform (z) was found to facilitate blood sample collection within the guide circle on the filter paper (see Figure 4A) instead of smearing outside its perimeter (see Figure 4B). In order to be able to quantify this, we have adopted the comparative dimensionless metric

$$f(r/R) = \frac{A(r)}{A_T}$$

where $A(r)$ is the area of blood impression located within radius r of the centre of the marked circle, A_T is the total area of the blood impression, and $R = 6$ mm is the radius of the marked circle.

Image processing programs were developed in in MATLAB (Mathworks) to quantitively measure blood impression distribution to determine comparative metric coefficients. Figure 5 shows the algorithm output for a given sample showing $A(r)$ highlighted in purple.

Figure 5 – Dried blood spot distribution program output

Figure 6A provides plots of the metric f for the blood impressions given in Figure 4A & Figure 4B against various values of r/R. With gyroscope stabilisation, it can be seen that at r/R = 1, a desirable value of f = 1 was obtained indicating that sample spot application was achieved completely within the guide circle. On the other hand, without stabilisation from the gyroscope, a lower f value of 0.8 was obtained at r/R = 1. In order to assess the reproducibility of the results, the same procedure was repeated for 7 spot applications with and without using the stabilisation platform. Figure 6B provides box plots of the distributions of f for r/R = 1 (based on 7 samples each) with the rocking mechanism operating under high (40°) and low (20°) angular amplitudes but at the same frequency (0.5 Hz), and with and without gyroscope stabilisation being introduced.
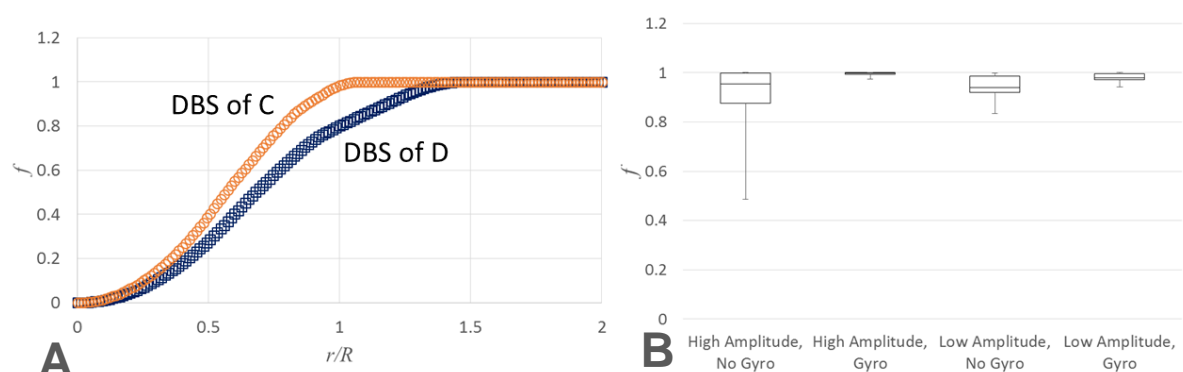

Figure 6 - Analysis of dried blood spot accuracy

The results clearly demonstrated the consistent good performance with gyroscope stabilisation notwithstanding the rocking amplitude that was being used. In the absence of the any stabilisation, high amplitudes of rocking, as expected, caused significantly higher inaccuracy and spread of the dried blood spot collected within the guide circle. An added benefit with the stabilisation was in allowing the practitioner to quickly spot the blood on the paper more readily, as opposed to some extra time and careful attention needed for targeting otherwise.

In summary, a cost-effective gyroscope stabilisation platform was demonstrated here to enable consistent and improved dried blood spot collection.

4. Simulating Motion of UAVs or Other Vehicles for Biochemical Sample Testing

4.1 Introduction

Transportation of biochemical samples continues to be an important factor in disease management and biochemical testing. The increased need for samples to be transported in rural areas has resulted in a variety of transportation methods used, including traversing unmade roads or using unmanned aerial vehicles (UAVs) to carry samples via flight. Methods such as these are often rough, and samples are subject to irregular motion that can result in sloshing and spillage.

A system was developed that is based on the use of MEMS based sensors incorporated in smartphones and the Arduino micro-controller to collect motion data in the field. This data is then relayed to a mechanical simulation platform designed and developed in order to be able to replicate the field motion faithfully. With the platform in operation, it is possible to test the effects of irregular motion on samples during transport without field testing, which can be resource consuming and avoid extensive licensing requirements in the case of UAV testing.

4.2 Field Data Collection

A data collection system was developed to collect the vibration and impact data from a vehicle that may be used to transport specimens. The system comprised of a LSM9DS0 inertial measurement unit, an ATmega328P microcontroller and a laptop computer.

The low-cost LSM9DS0 IMU used includes 3-axis accelerometers, 3-axis gyroscope and 3-axis magnetometer, totalling 9 degrees of freedom (DoF). Data from individual sensors are combined using 9-DoF Madgwick fusion algorithms to determine the roll, pitch and yaw of the sensor which are then stored in a spreadsheet on a laptop computer. It was necessary to use a 9-DoF sensor to prevent drifting yaw measurements by using the magnetometer readings as a reference. The IMU is operated using the ATmega328P, which has been programmed to implement Madgwick fusion algorithms.

4.3 Motion Simulation Platform

The simulation system developed involved a platform capable of moving with six degrees of freedom: the linear movements (lateral, longitudinal and vertical), and three rotations (pitch, roll and yaw). The 6-DoF control of this system (as opposed to the rocking platforms 1-DoF) is able to accurately replicate motion of various types of vehicles. The simulation system is comprised of three parts: a Stewart platform, motion controller board, and motion driver software.

A Stewart platform (also known as a hexapod platform) was constructed using 6 servomotors positioned shown in Figure 7. Two linkages attached to each servomotor allows the platform to be controlled with six degrees of freedom. The movement of the platform is constrained by the linkage lengths, as such it is limited to motion in all 6-DoF. However, the platform movement is sufficient to replicate vehicular motion, as they do not experience large changes in pitch and roll during regular motion.

Figure 7 – 6-DoF Stewart platform arrangement with 6 servomotors

The AMC1280USB motion controller board was used to control the Stewart platform servomotors. The controller acted as the actuator position close loop control in the system, connecting motion driver software data to actuator (servomotor) movement. The board powers and controls all 6 servos to the actuator position specified by the motion driver software.

Existing 6-DoF BFF Motion Driver software was used to control the platform simulator. With the platform measurements specified, the software is able to apply the inverse kinematics required to convert desired 6-axis motion data to actuator output. The software can be operated in two modes, one uses motion data from flight simulators or other simulation

games, while the other is used to manually receive motion data specified by an external program.

4.4 Simulator Kinematics

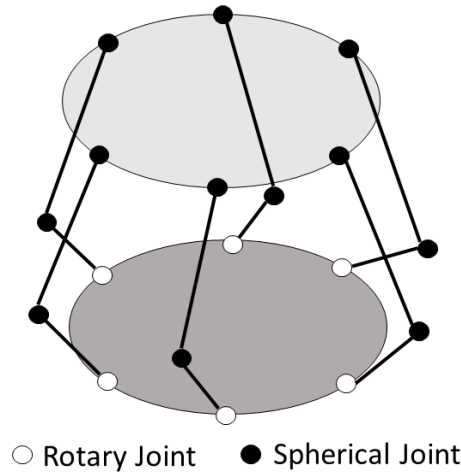The 6-DoF simulator developed is based on the use of revolute and spherical joints (Figure 8).

○ Rotary Joint   ● Spherical Joint

Figure 8 – Stewart Platform Joints

The base and platform origins are defined by the respective orthogonal Cartesian coordinates *x*, *y*, *z* and *x'*, *y'*, *z'*. Since the base is stationary, the platform origin has three displacement components with respect to the base. However, it will be more convenient to convert this to three rotations about the origin of the base; ψ (yaw) about the *z*-axis, θ (pitch) about the *y*-axis, and φ (roll) about the *x*-axis. The transformation matrix *R* that relates the coordinates on the base to that of the platform via:

$$\begin{bmatrix} x \\ y \\ z \end{bmatrix} = R \begin{bmatrix} x' \\ y' \\ z' \end{bmatrix}$$

(1)

This matrix is the product of the respective yaw $R(\psi)$, pitch $R(\theta)$, and roll $R(\varphi)$ matrices, such that:

$$R = R(\psi) \cdot R(\theta) \cdot R(\varphi)$$

$$= \begin{pmatrix} \cos\psi & -\sin\psi & 0 \\ \sin\psi & \cos\psi & 0 \\ 0 & 0 & 1 \end{pmatrix} \cdot \begin{pmatrix} \cos\theta & 0 & \sin\theta \\ 0 & 1 & 0 \\ -\sin\theta & 0 & \cos\theta \end{pmatrix} \cdot \begin{pmatrix} 1 & 0 & 0 \\ 0 & \cos\varphi & -\sin\varphi \\ 0 & \sin\varphi & \cos\varphi \end{pmatrix}$$

$$= \begin{pmatrix} \cos\psi\cos\theta & -\sin\psi\cos\varphi + \cos\psi\sin\theta\sin\varphi & \sin\psi\sin\varphi + \cos\psi\sin\theta\cos\varphi \\ \sin\psi\cos\theta & \cos\psi\cos\varphi + \sin\psi\sin\theta\sin\varphi & -\cos\psi\sin\varphi + \sin\psi\sin\theta\cos\varphi \\ -\sin\theta & \cos\theta\sin\varphi & \cos\theta\cos\varphi \end{pmatrix}$$

(2)

Let us suppose that joints on the base B_i and platform P_i are considered (see Figure 9(a)). T is the translation vector that gives the positional linear displacement of the origin of the platform O' from the origin of the base O. If b_i is the translation vector of O to B_i, and p_i is the translation vector of O' to P_i, then the vector l_i from B_i to P_i can be expressed as:
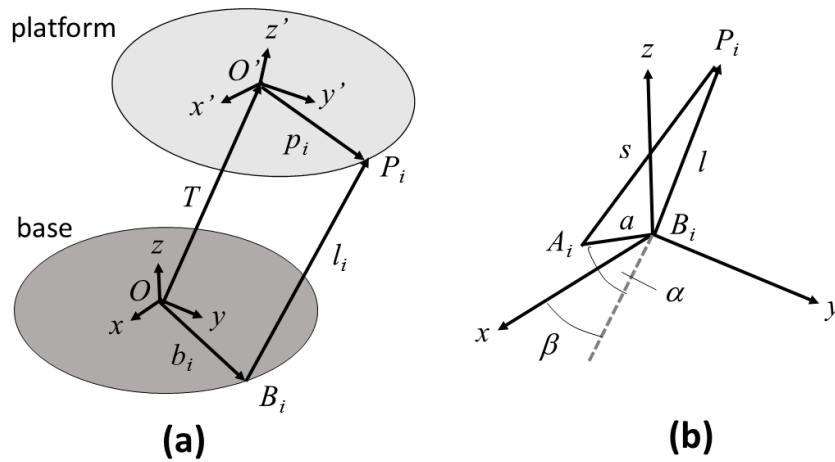
$$l_i = T + (R \cdot p_i) - b_i$$

(3)

Figure 9 – Platform Kinematics

Further calculation is needed in order to find the rotations needed at revolute joint B_i (see Figure 9(b)). Naturally, the length of arms $B_i A_i$ and $A_i P_i$ are fixed. At B_i, suppose that β is the rotational angle from the x-axis, and α the rotational angle from the x-y plane. If the coordinates of B_i and A_i are (x_B, y_B, z_B) and (x_A, y_A, z_A) respectively, they are related to each other via:

$$x_A = a\cos\alpha\cos\beta + x_B$$
$$y_A = a\cos\alpha\sin\beta + y_B$$
$$z_A = a\sin\alpha + z_B$$

(4)

where a is the fixed length between B_i and A_i. If the distance between A_i and P_i is s, applying Pythagoras theorem gives us:

$$a^2 = (x_A - x_B)^2 + (y_A - y_B)^2 + (z_A - z_B)^2$$
$$s^2 = (x_P - x_A)^2 + (y_P - y_A)^2 + (z_P - z_A)^2$$
$$l^2 = (x_P - x_B)^2 + (y_P - y_B)^2 + (z_P - z_B)^2$$

(5)

Since the coordinates of B_i are known, there coordinates of B_i and P_i as well as I are unknown. For any translation, yaw, pitch, and roll of the platform relative to the base, it will be possible to establish I_i from Eq. (3) and thus the coordinates of P_i from Eq. (5). Since β is known, it will be possible to determine α and thus the rotation of the arm that is connected to the motor at B_i.

4.5 Results and Discussion

The sensor used to collect field data was mounted to the dashboard of a Mitsubishi Outlander (see Figure 10) to record vibration and impact information for a variety of land-based transport terrains. Motion data was recorded for short durations in areas with the following characteristics: uphill, downhill, dirt road, bumpy and humps. The various datasets were chosen to allow the simulator to accurately replicate vehicular motion in all land-based circumstances by testing datasets independently or by using combinations of multiple terrains.

Figure 10 - Field data collection system

In addition to the IMU sensor, it was shown that a smartphone can also be used to collect vibration and impact information when placed inside a vehicle. Figure 11 shows acceleration measurements using the IMU sensor and smartphone as both were placed on a platform and subjected to identical perturbations. It is clear that the measurements are highly correlated, which indicates that either device could be used to obtain good measurements when placed inside a vehicle. It is noteworthy that the smartphone used offers 10Hz, whereas the IMU operates at 100Hz. High sample rate is desirable for vibration collection, but for impact tests 10Hz is sufficient. A typical Samsung Galaxy SIII smartphone retails for US$225 as opposed to the IMU sensor board (and Arduino processor) which is available for

US$50. However, a smartphone may be already available to a user which can be used to collect data instead of an IMU sensor.
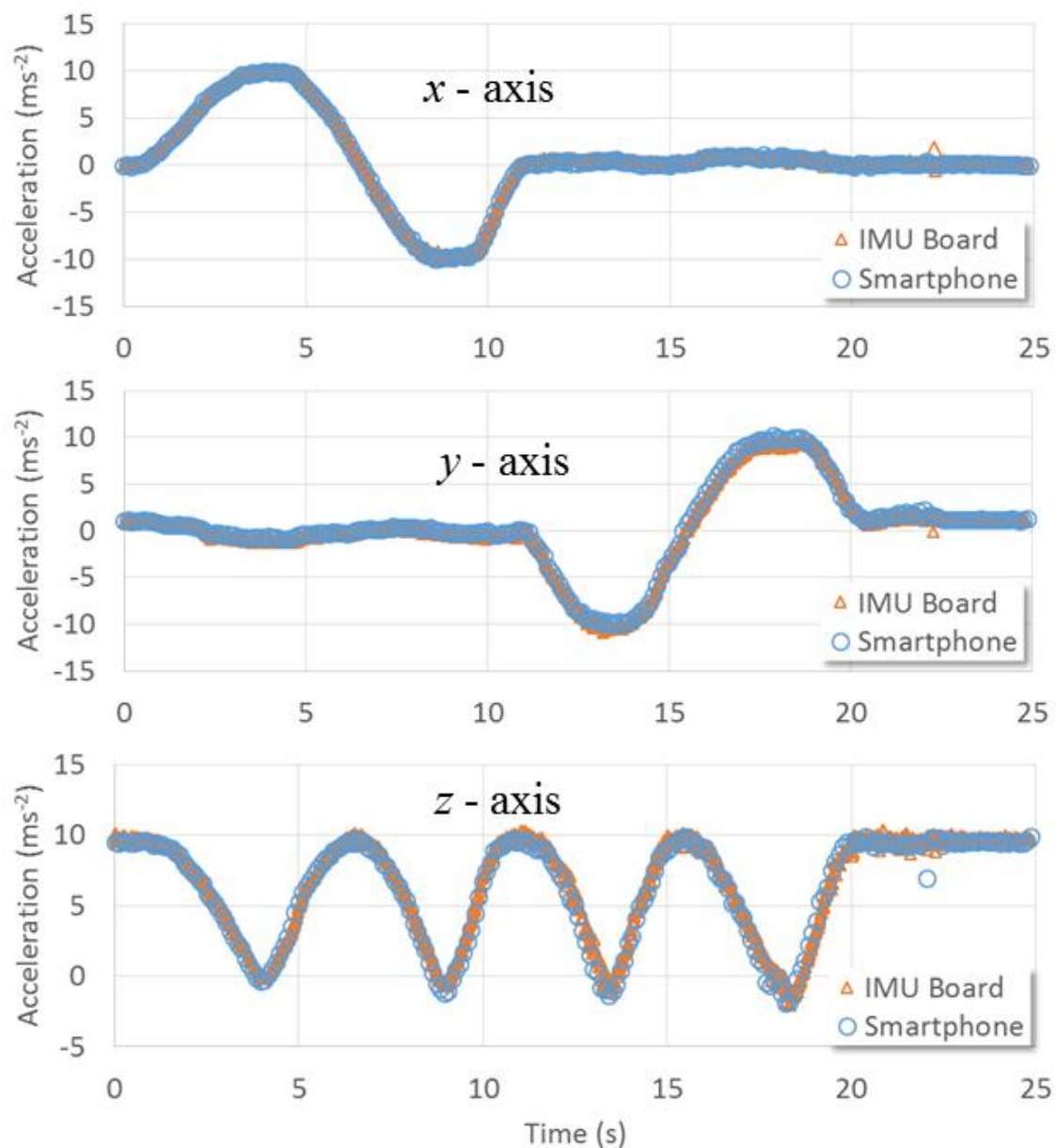

Figure 11 - Comparison of Phone and IMU Orientation Data

A program written in C++ was developed to transmit pre-recorded motion data from a file to the motion driver software. Data extracted from the file included a timestamp, acceleration readings (X, Y & Z) and orientation (yaw, pitch & roll). This data was encapsulated in UDP packets that were transmitted to the driver at 100Hz. Packet transmission timing was constrained using the timestamps, to ensure data was processed by the motion driver at the correct speed.

Figure 12 shows the operation of the Stewart platform using a set of data recorded in bumpy terrain. The plots show the orientation of the simulator and vehicle that was recorded during

motion. The ability of the simulator to replicate the vehicle's motion is shown to be quite accurate. However, small discrepancies are evident which result from a number of factors. Both sets of data were recorded using the same IMU device, but in different environments. The noise in each environment is different and may contribute to irregularities. Furthermore, the servomotors used in the platform are controlled using a digital pulse width modulation signal; resulting in a resolution of approximately 0.1 degrees. As each movement is comprised of several servomotor adjustments, the platform is unable to perform as smoothly as the vehicles it replicates.
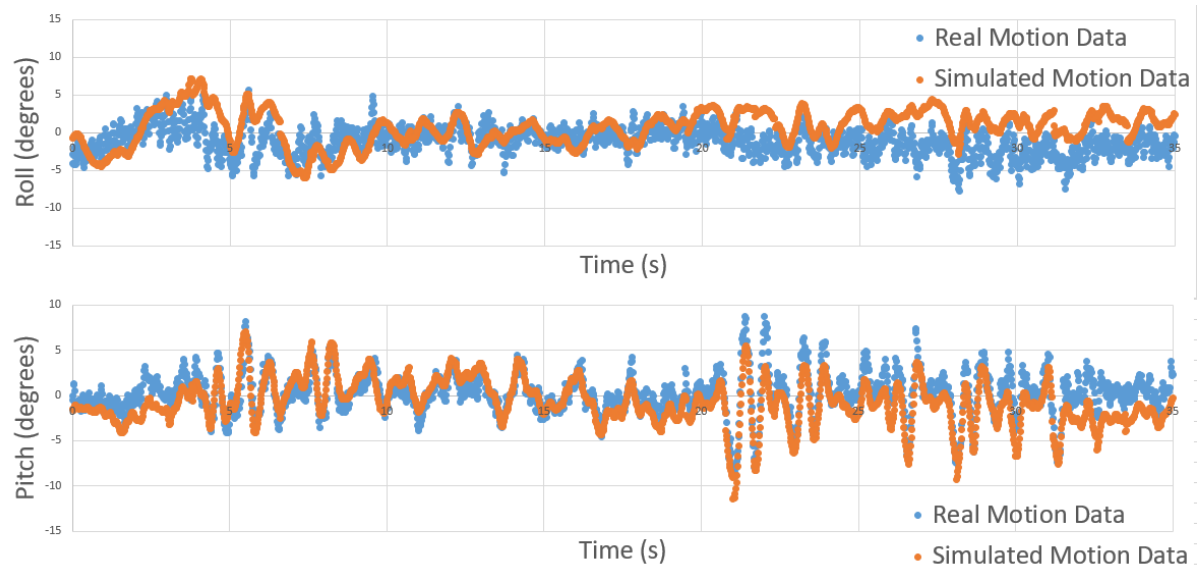

Figure 12 – Simulated motion output

The motion simulator was used to test the effects of transit on unpasteurised milk. When transported, unpasteurised milk can be damaged from vibrations and movement [71], resulting in a drop in pH level which can cause unwanted effects such as curdling. The simulator is able to test the effects of motion on the milk using realistic movement patterns. Initial results showed that the pH level of unpasteurised milk placed in small vials (Figure 13A) dropped by 0.05pH when placed on the simulator for two hours (Figure 13B).
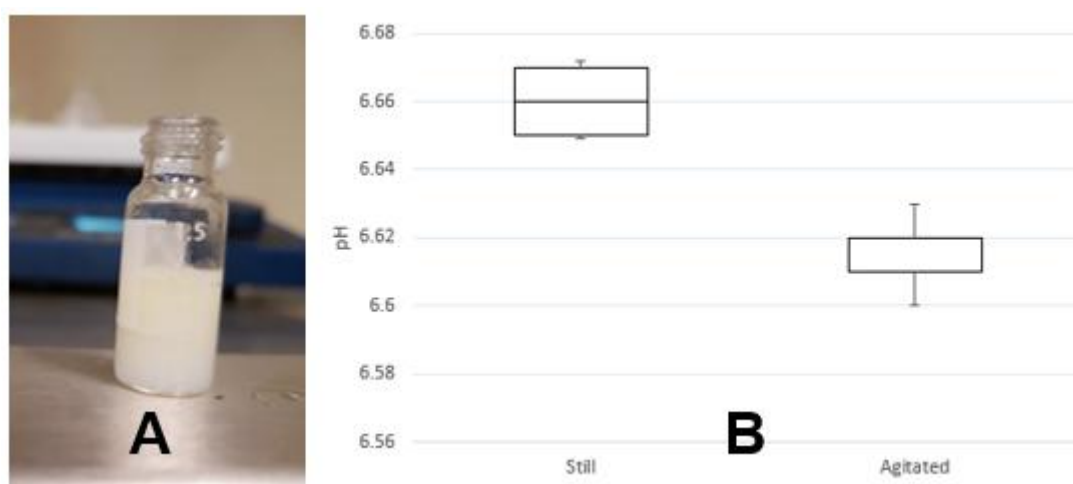
Figure 13 - Effects of motion on unpasteurised milk vials

Further tests were repeated on a following day to compare the effects of varying degrees of motion on samples placed in vials as well as small bags. To replicate various intensities of motion, acceleration and angles measured from real motion data were modified to investigate the difference in pH under different conditions of motion. A low amplitude was used to replicate relatively smooth motion by reducing measured movement by half. High amplitude tests involved increasing motion by double to further emphasise rough motion. In addition to vials, some milk samples were placed in small bags to test effects of different container volumes and shapes.
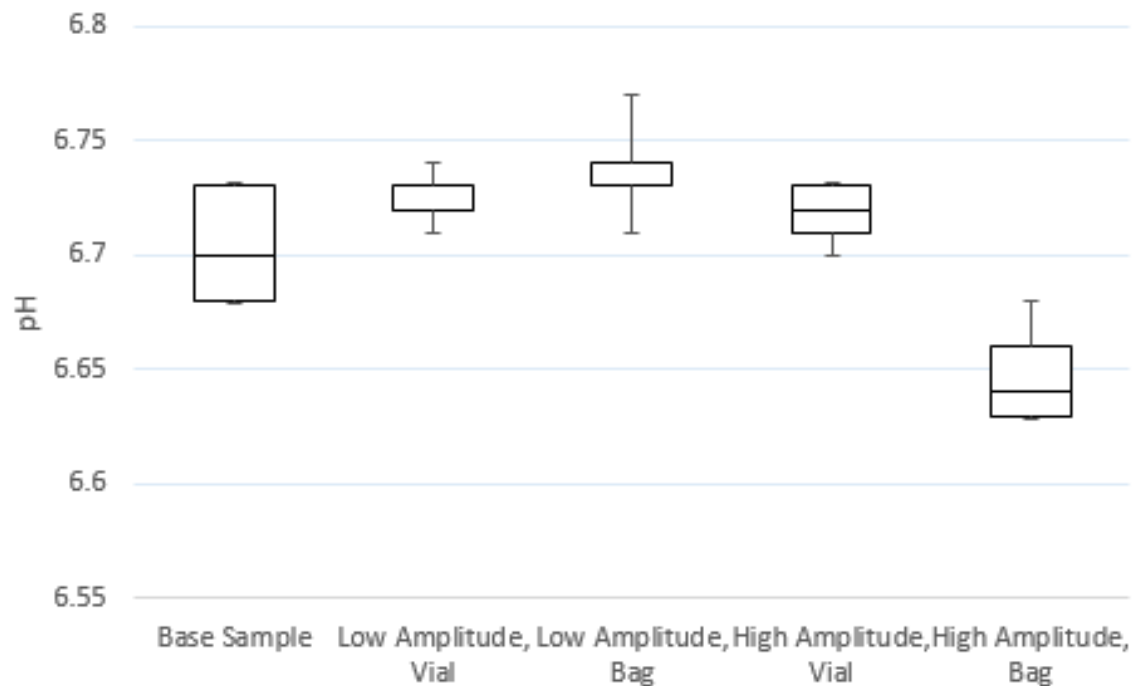

Figure 14 – Effects of high and low amplitude motion on unpasteurised milk in different containers

The results in Figure 14 show no significant change to pH under low amplitude motion, and up to 0.06 pH reduction when samples were placed in bags under high amplitude motion. These results show no significant increase from initial tests with vials, however small differences may be noted due to small changes to milk samples and environment conditions between the two tests.

The reduction in pH from the simulations was much smaller than described in previous works[71]. This may be caused by different varieties of milk or the method used to agitate samples. In previous studies, samples were oscillated in a regular pattern, which does not replicate realistic transport methods. The oscillating pattern may have resulted in more significant damage to the samples due to sloshing which caused the pH to drop further. Furthermore, changes in temperature due to the testing environment or kinematic energy may also contribute to pH alterations.

There are a variety of applications in which it is advantageous to simulate motion in a laboratory instead of field testing. The simulation system developed is able to accurately replicate vibration and impact information recorded from a vehicle during transit. This system provides more accurate tests to be performed in laboratories, such as milk transportation, where results from realistic motion differ from synthetic oscillations. This system is the first effort reported that provides reproductions of movements of real-world transport conditions in the laboratory in order to derive reliable data that correlates the effect of motion on the quality of liquid samples.

5. The Effects of Gusts on Small Unmanned Aerial Vehicles

5.1 Introduction

Small unmanned aerial vehicles have become increasing popular due to their cost and availability. However, for aspects in biochemical field processes such as transport and surveying, quadcopter type UAVs are often quite expensive energetically. Balloon UAVs make use of buoyancy to aid flight, resulting in a slower but stable alternative. However, slow flying UAVs such as these are often affected by wind dynamics such as gusts.

Testing the effects gusts on small UAVs in the field can be difficult due to licensing and the uncontrolled environment. A gust simulator allows testing to be performed in a controlled environment, while maintaining capabilities to generate turbulence experienced by UAVs during flight. This allows UAVs to be tested in different wind speeds to investigate ways to improve stability for purposes such as surveying.

5.2 Gust Simulator

The gust simulator was designed and built to work within the test section of a wind tunnel (which had a cross section of 1m x 1m) (see Figure 15). Hence, its dimensions were smaller, although the extent of the reduction is marginal. The operation is based on the principle that when the vanes at the front of simulator are closed (B), the space within it undergoes a lull flight condition. However, as soon as they are opened (C), a gust condition is introduced, in which the duration can be controlled until the vanes are closed again. All sides of the chamber are closed except for its rear (downstream to the airflow) to ensure that no stagnation in the airspace occurs when the gust condition is at play.
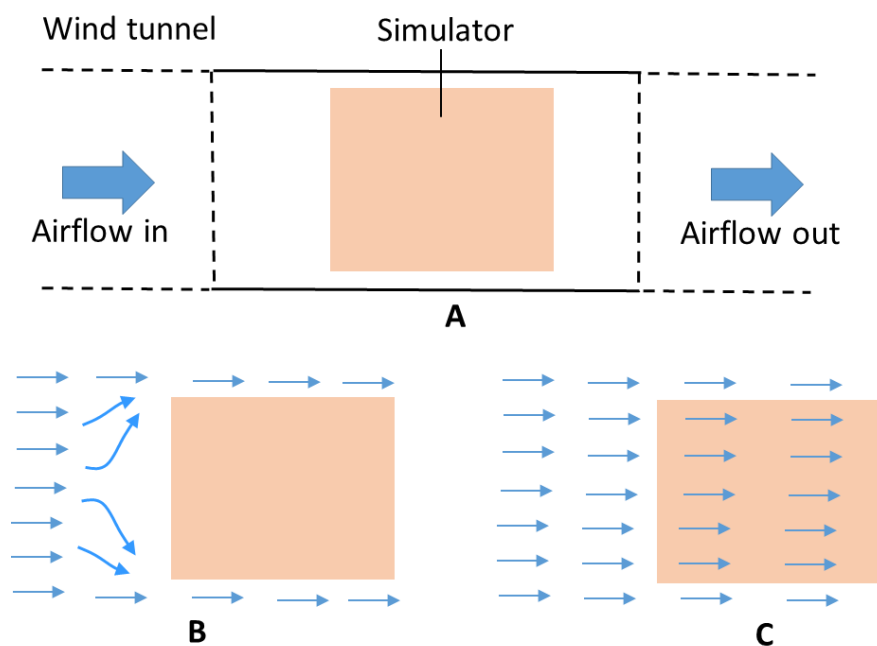

Figure 15 – Wind tunnel airflow with moveable simulator

The most convenient construction is for the vanes to be arranged orthogonal and in a straight row to oppose the flow when in the closed position. This however creates separation flows over the bluff body that results in high drag (drag coefficient ~ 2 if taken as a 2D case) as well a large stagnation flow region upstream of the vanes. The latter can present issues when the vanes are opened suddenly opened to try to simulate a gust.

The simulator developed here (Figure 16) overcomes this problem by having the vanes organised in the form of a circular arc. This reduces the drag considerably (drag coefficient ~ 1.2 if taken as a 2D case) and reduces the stagnation region upstream of the vanes when they are closed. The simulator has dimensions of L = 61cm, H = 45cm, and W = 53cm. The opening and closing of the vanes is attained using servomotor actuation, coordinated by a micro-controller (Arduino Uno). Two of closed sides comprise transparent plexiglass plates to enable viewing and the LED lighting is incorporated to provide clearer image recordings.
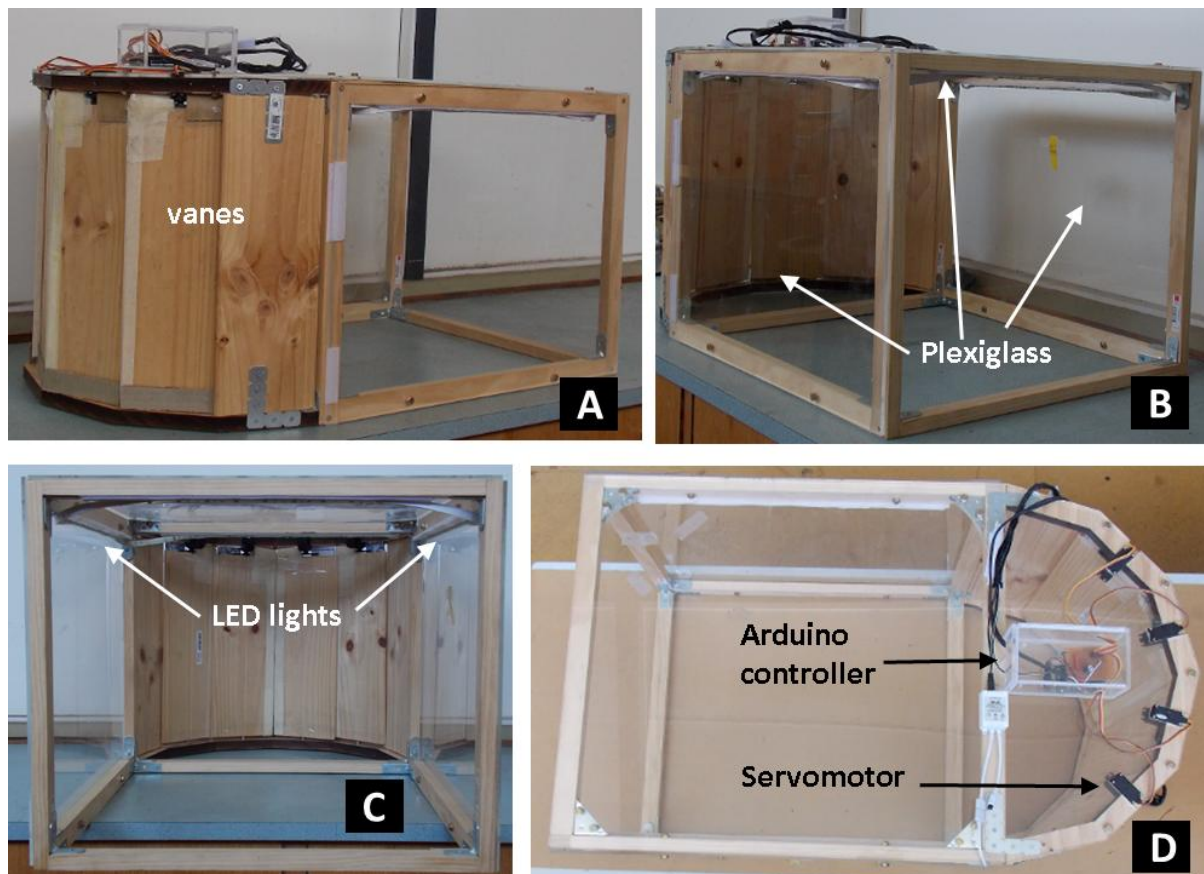

Figure 16 – Gust simulator

5.3 Results and Discussion

The gust simulator was mounted inside the wind tunnel and tested at various wind speeds. A Modern Device Rev. C digital wind sensor was used injunction with an Arduino microcontroller to record wind speeds inside the simulator. The simulator was opened for a period of 30 seconds to allow wind speed measurements to stabilise before closing the front vanes. This was repeated 5 times at each speed setting to verify consistency. The

measurements from this test are shown in Figure 17, where the wind tunnel was operated at 5 different speeds; ranging from 2kph up to 24kph. The results show consistent wind speed at different speed settings, with less consistency at low operating speeds.
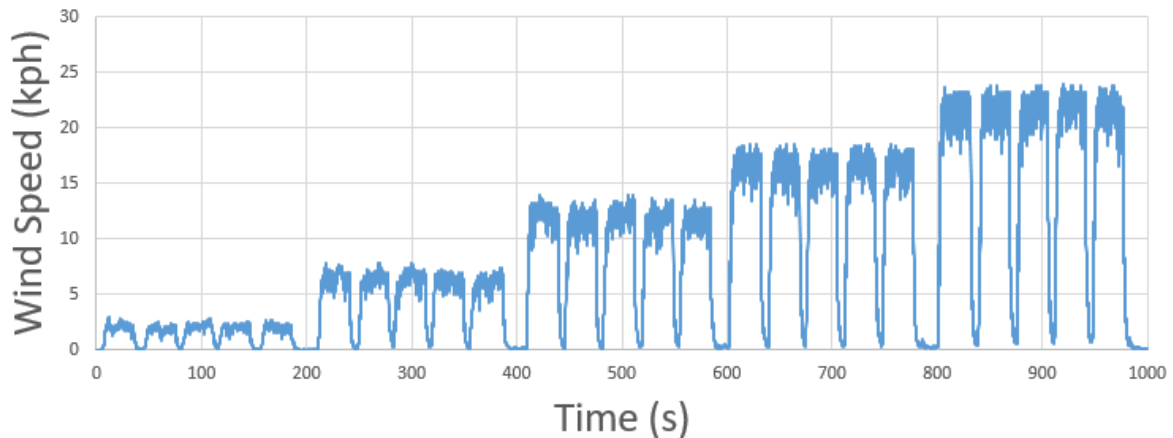

Figure 17 – Wind speed measurements inside gust simulator

Figure 18 below shows the wind speed measuring inside the simulator during a high speed gust. There is a 3.5 second rise time from when the vanes are opened to when the full speed is measured inside the simulator. During the period when the gust simulator is at maximum speed, there are small variations to wind speed likely due to minor pressure differentials which is unlikely significant except for at smaller speeds when variations are more proportional to operating speeds. After vanes are closed, the wind speed takes approximately 5 seconds to drop to zero. The ability to achieve zero wind speed allows for quiescent environment to be created between simulated gusts.

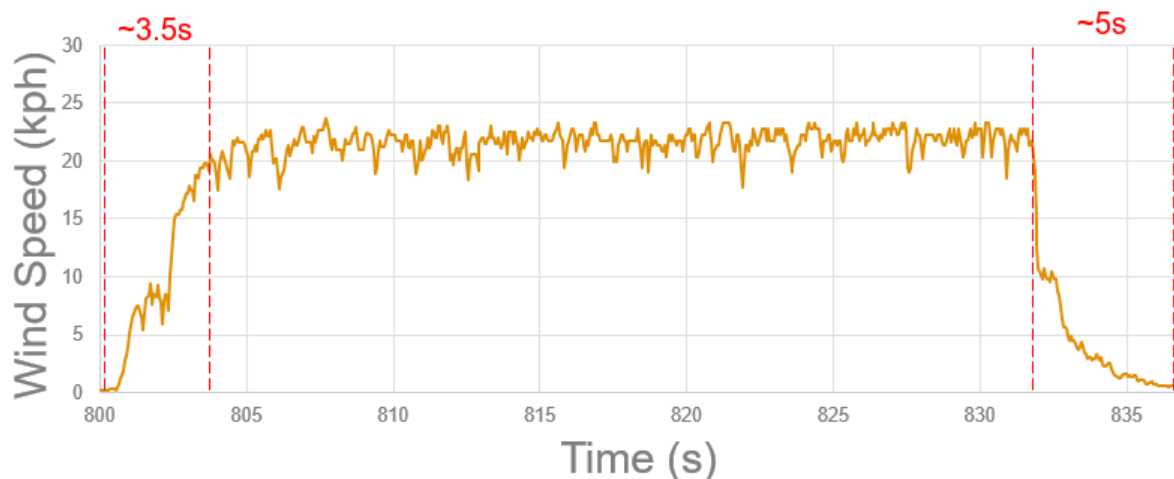*Figure 18 – Wind speed measurements during simulation gust*

To test the effects of gusts on balloon UAVs, a balloon was introduced to the gust simulator as shown in Figure 19. The balloon was filled with helium to a diameter of 28cm. A LSM9DS0 IMU sensor was attached to the base of the balloon, from which information of the yaw, pitch and roll were extracted using an Arduino Uno controller. Additional mass was

added to the balloon to balance the weight of the device with the upward buoyant force. The balloon was able to hover in the gust simulator, mimicking a balloon UAV in hover mode which was unable to be operating in the confined space of the simulator.
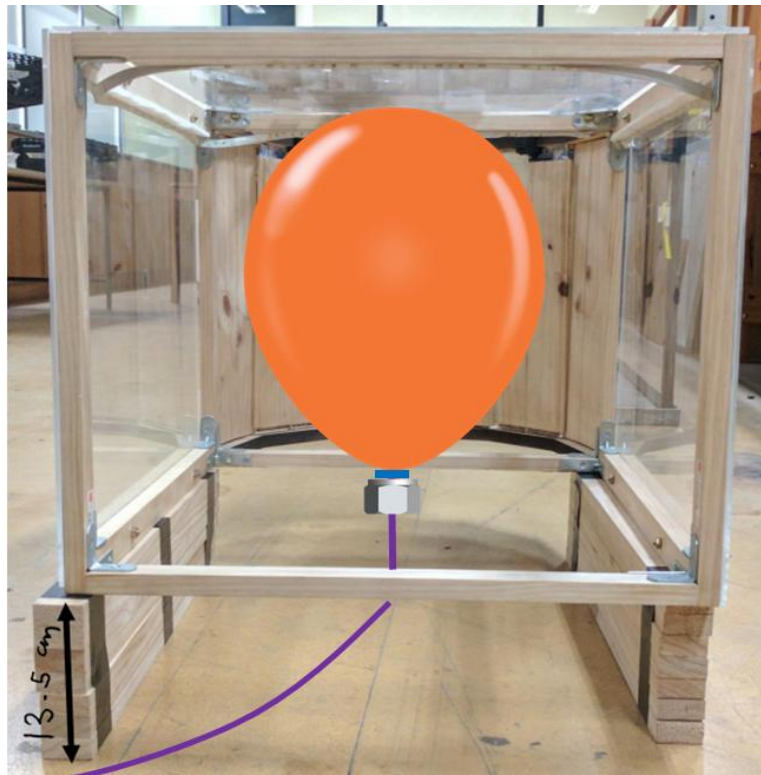

Figure 19 - Gust simulator set up for balloon UAV simulation

The wind tunnel was operated at speeds below 3kph to ensure the hovering balloon remained centered in the simulator. The gust simulator was opened for 30 seconds at each speed for stability, which was then repeated 5 times for consistency. Figure 20 shows the orientation of the balloon during a gust simulation with low wind speeds of 2.5kph. At low air speeds, the impact of the gust on the balloon has little effect on roll and pitch of the balloon. However, the significant changes to yaw are evident even at low speeds. When the front vanes are closed, a large fluctuation in yaw occurs due to the sudden decrease in pressure at the front of the simulator.
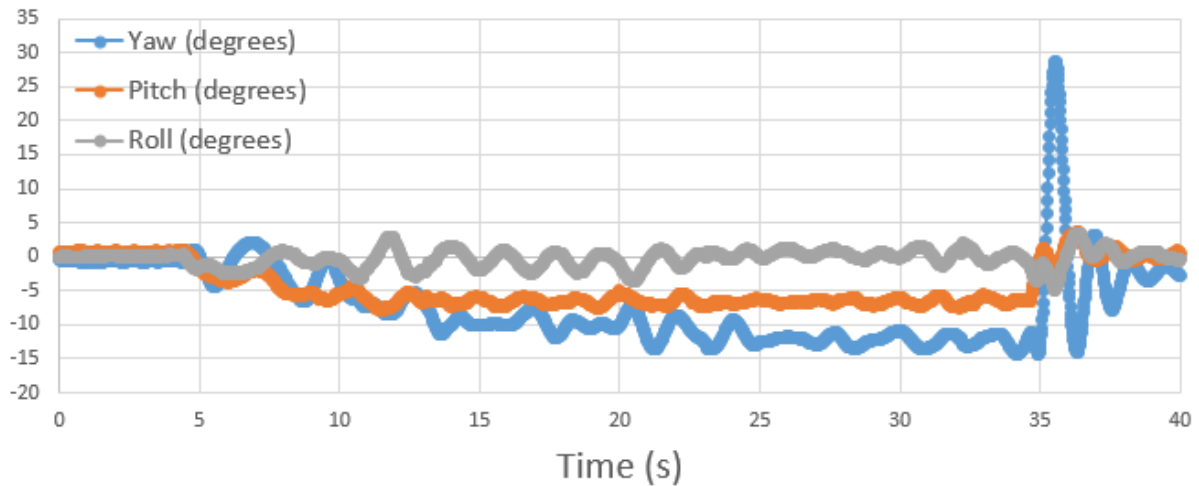
Figure 20 – Balloon dynamics during small simulated gusts

The results suggest that balloon UAVs are more disposed to perturbations in yaw compared to pitch and roll. Large rotations observed may have resulted due to inaccurate IMU placement. It is essential that weight is evenly distributed around the center of the balloon, as mall changes in weight distribution may result in large rotations due to wind.

For surveying purposes, changes in yaw will reduce the field of view if yaw is left unaccounted for until post-processing of images. To prevent this, a light-weight mechanism can be attached to the UAV to provide yaw stabilisation. Alternatively, different shapes of balloons with non-uniform airflow characteristics will greatly reduce fluctuations in yaw and provide more stable positioning for robust surveying.

The movements of the balloon UAV are currently coordinated using a manual steering controller. In order to attain active correction to the effects of pitch, roll, and yaw due to gust, it will be necessary to first develop an autonomous system and then implement the programmed interventions to do so. This is an ongoing effort that is beyond the scope of this project.

6. Spillage Prevention in Biochemical Laboratories

6.1 Introduction

In the biochemical laboratory, samples are almost always liquids transported in microplates. In using robotic automated systems to handle microplates, the avoidance of liquid spillage during transport can often be more important than high precision position and velocity control. Spillage can come about either when the liquid receptacle is subjected to inadvertent collision or tilted excessively. An approach of incorporating low-cost IMUs to an equally low-cost SCARA was developed to create a system capable of sensing collision and determining the amount of tilt. Based on this, the system will raise an alarm, abandon its current operation, and return to its original position when any collision or excessive tilting is detected. A method to predict the location of any obstacle that causes a collision, based on the trajectory of the robotic arm as well as the acceleration feeds in the IMU, is also demonstrated.

6.2 Interfacing with a Low-cost Robotic Arm

In this system, the low-cost SCARA used was the AL5D from Lynxmotion. The arm is driven by a series of servomotors located at the base, shoulder, elbow, wrist, and gripper respectively. In order to accommodate the ability to transport microplates, the gripper range was extended by incorporating adaptors.
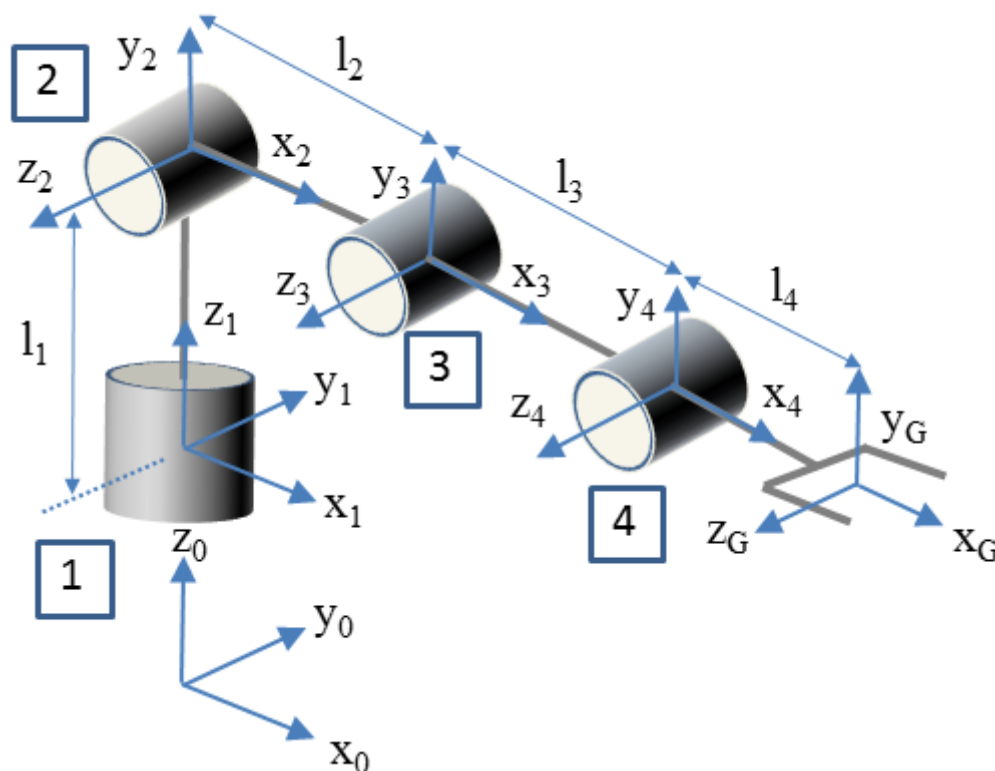

Figure 21 - Robot arm axis structure

The robotic arm was used under 4 degrees of freedom (see Figure 21). Standard Denavit-Hartenberg notation was used to depict the forwards kinematics of the manipulator [72]. With this, the transformation matrices between consecutive links are:

$$
{}^{0}T_{1} = \begin{pmatrix} \cos\theta_1 & -\sin\theta_1 & 0 & 0 \\ \sin\theta_1 & \cos\theta_1 & 0 & 0 \\ 0 & 0 & 1 & l_1 \\ 0 & 0 & 0 & 1 \end{pmatrix} \quad {}^{1}T_{2} = \begin{pmatrix} \cos\theta_2 & -\sin\theta_2 & 0 & 0 \\ 0 & 0 & -1 & 0 \\ \sin\theta_2 & \cos\theta_2 & 0 & 0 \\ 0 & 0 & 0 & 1 \end{pmatrix} \quad {}^{2}T_{3} = \begin{pmatrix} \cos\theta_3 & -\sin\theta_3 & 0 & l_2 \\ \sin\theta_3 & \cos\theta_3 & 0 & 0 \\ 0 & 0 & 1 & 0 \\ 0 & 0 & 0 & 1 \end{pmatrix}
$$

$$
{}^{3}T_{4} = \begin{pmatrix} \cos\theta_4 & -\sin\theta_4 & 0 & l_3 \\ \sin\theta_4 & \cos\theta_4 & 0 & 0 \\ 0 & 0 & 1 & 0 \\ 0 & 0 & 0 & 1 \end{pmatrix} \quad {}^{4}T_{G} = \begin{pmatrix} 1 & 0 & 0 & l_4 \\ 0 & 1 & 0 & 0 \\ 0 & 0 & 1 & 0 \\ 0 & 0 & 0 & 1 \end{pmatrix}
$$

(6)

With these matrices, simple sequential multiplication allows the base to be linked to the gripper using:

$$
{}^{0}T_{G} = {}^{0}T_{1}\,{}^{1}T_{2}\,{}^{2}T_{3}\,{}^{3}T_{4}\,{}^{4}T_{G}
$$

(7)

The robotic arm was controlled using an ATmega328P single board microcontroller (Arduino Uno), programmed to control all 5 servomotors using pulse width modulation (PWM). Inverse kinematics equations Eq. (8) were used to allow linear movement of the robotic arm in a cylindrical coordinate system by determining the angles (θ_1, θ_2, θ_3, θ_4) required to position the gripper at (x_G, y_G, z_G) (see Figure 22). Since the liquid sample must be held without spillage, the gripper angle (θ_G) needs to be constrained to remain constantly perpendicular to the global *x-y* plane.

$$
\theta_1 = \tan^{-1}\left(\frac{y_G}{x_G}\right) \quad \theta_2 = \alpha + \beta \quad \theta_3 = \cos^{-1}\left(\frac{l_2^2 + l_3^2 - l_{24}^2}{2l_2 l_3}\right) \quad \theta_4 = \theta_G - \theta_2 - \theta_3 \quad \theta_G = \tan^{-1}\left(\frac{z_G - z_4}{r_G - r_4}\right)
$$

$$
r_G = \sqrt{x_G^2 + y_G^2} \quad r_4 = \sqrt{x_4^2 + y_4^2} \quad l_{24} = \sqrt{r_{24}^2 + z_{24}^2} \quad r_{24} = r_G - l_4 \cos\theta_G \quad z_{24} = z_G - l_1 - l_4 \sin\theta_G
$$

$$
\alpha = \tan^{-1}\left(\frac{z_{24}}{r_{24}}\right) \quad \beta = \cos^{-1}\left(\frac{l_2^2 - l_3^2 + l_{24}^2}{2l_2 l_{24}}\right) \tag{8}
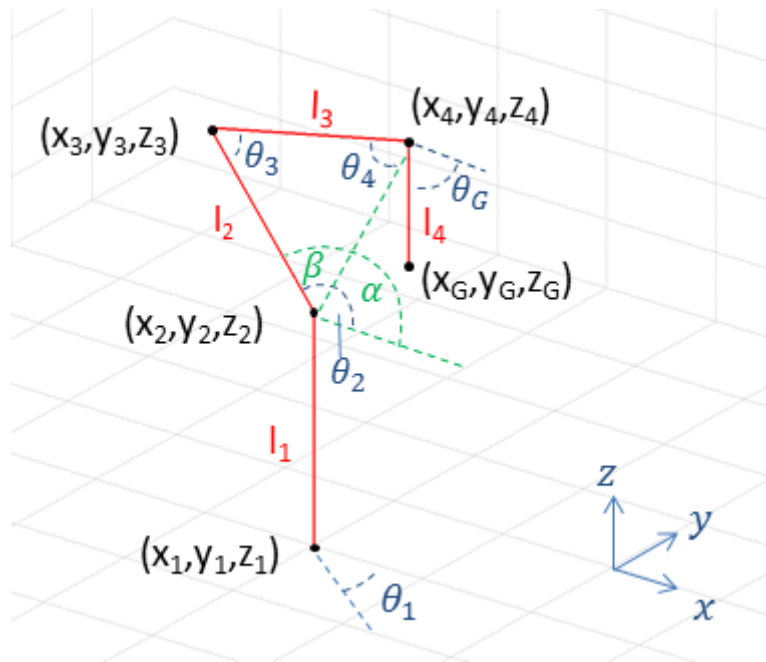$$

Figure 22 – Coordinate system for simulation and collision detection

The low-cost servomotors used in the robotic arm are very basic, with simple circuitry that compares the pulse width of the input signal with a position-dependant potentiometer resistance. As such they have no integrated speed control or feedback. To indirectly control the rotational speed of servomotors it is possible to implement a delay between small changes in position, sweeping from one position to the destination through discrete steps at a controlled speed. Improvements were made to this method by varying the delay between steps sinusoidally, producing smoother movement to further reduce chance of spillage.

6.3 Accelerometer and Inertial Measurements Unit Interfacing

To reduce the probability of spillage in the biochemical laboratory attempts were made to monitor the rotation of robot arm linkages. There are a variety of ways to measure rotation, which then allows the amount of tilt to be determined and collisions to be detected. An inexpensive but effective approach to measure the relative rotation between two linkages is via the use of optical rotary encoders or potentiometers. However, since actuators are used to rotate the arms of a SCARA, it is generally difficult to locate these sensors there as well to determine the amount of tilt. Actuators such as servomotors have potentiometers built inside them to provide information on the extent of rotation based on a reference unlike stepper motors. However, this method was inaccurate, especially during collisions. In theory, it is also possible to use accelerometers to measure rotation by referencing to the constant gravitational acceleration vector. However, this method can only determine the pitch of the linkage and is not expected to produce accurate rotation measurements when the robotic arm is in movement.

To overcome inaccuracies caused by fluctuation accelerometer readings under motion, inertial measurement units were used. The low-cost LSM9DS0 IMU used includes 3-axis

accelerometers, 3-axis gyroscope and 3-axis magnetometer, totalling 9 degrees of freedom (DoF). Data from individual sensors are combined using 9 DoF Madgwick fusion algorithms to determine the roll, pitch and yaw of sensor-attached linkages. As previously mentioned, it was necessary to use a 9 DoF to prevent drifting yaw measurements by using the magnetometer readings as a reference. The IMU is also operated using the ATmega328P, which has been programmed to implement Madgwick fusion algorithms.

6.4 Results and Discussion

The IMU was attached to the robot arm which was used to transport microplates as shown in Figure 23. The IMU attached to the linkage l2 produced rotational measurements θ_1 (yaw) and θ_2 (pitch) with a mean absolute error (ε) of 1.70° and standard deviation (σ) of 1.77.
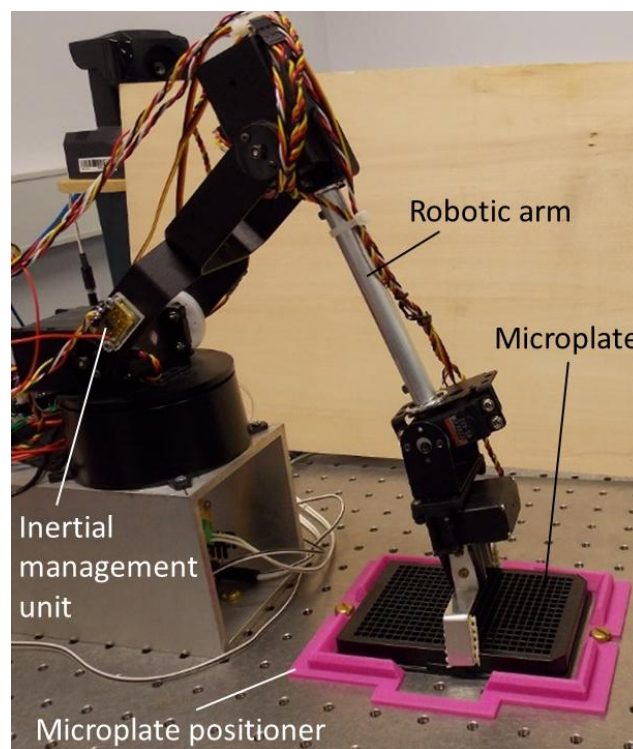

Figure 23 – Robotic arm setup with inertial measurement units used to pick up microplates

Whilst consistently accurate at most angles, it was observed to produce errors of over 5° at horizontal extremities. Due to this limitation, the IMU was deemed inappropriate for direct positional feedback for control systems. However, as the servomotors contain internal feedback circuitry the only circumstance resulting in a disparity between the anticipated linkage angle and the actual measured angle is when the arm has been influenced by external factors, such as a collision. In this scenario, the IMU is able to detect this disparity so it is able to detect collisions and implement collision management procedures. This was tested by sweeping the servo in the horizontal plane and simulation a collision mid-sweep (see Figure 24).
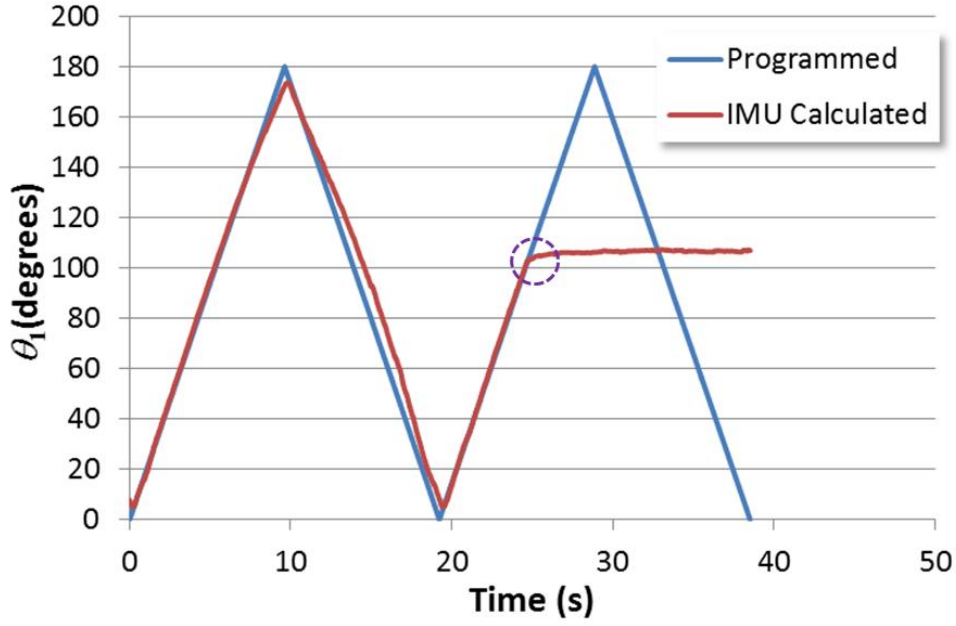
Figure 24 - Using IMU outputs to identify collisions (shown in purple)

The angle used to detect collisions is the angle between the anticipated linkage position and the calculated linkage position can be denoted as δ. If $\bar{\theta}_1$ and $\bar{\theta}_2$ are the anticipated angles of the robotic arm, it is possible to express all these parameters using:

$$\cos(\delta) = \cos\left(\theta_1 - \bar{\theta}_1\right)\cos\left(\theta_2\right)\cos\left(\bar{\theta}_2\right) + \sin\left(\theta_2\right)\sin\left(\bar{\theta}_2\right)$$

(9)

The collision detection angle (δ) is measured periodically when the robotic arm is in motion, and if it is calculated to be larger than a set threshold (δ_{th}) then a collision has been detected. The current collision management procedure involves retracting the robot arms movement to the previous safe position but could also alert operators of the collision and wait for manual intervention.

Collision simulation based on this method was developed using MATLAB. The simulation was developed to demonstrate the ability of the IMU collision detection system to estimate the position that the collision occurred. The simulation assumes that the robotic arm moves linearly in a cylindrical coordinate system (constant Δr, Δϕ and Δz). This means the trajectory of the robot arm can be easily calculated given the start and end points of travel. The alternative method of storing previous locations was not used due to ATmega328P memory limitations.

A threshold of $\delta_{th} = 2.5\sigma$ was used for this simulation ($\sigma = \sigma_1 = \sigma_2$), such that the probability of the estimated position lying outside the acceptance region is very low. While the robot arm moves along the travel path the red area shows the possible position of the robot arm given that δ has been calculated to be outside the acceptance region (Figure 25).
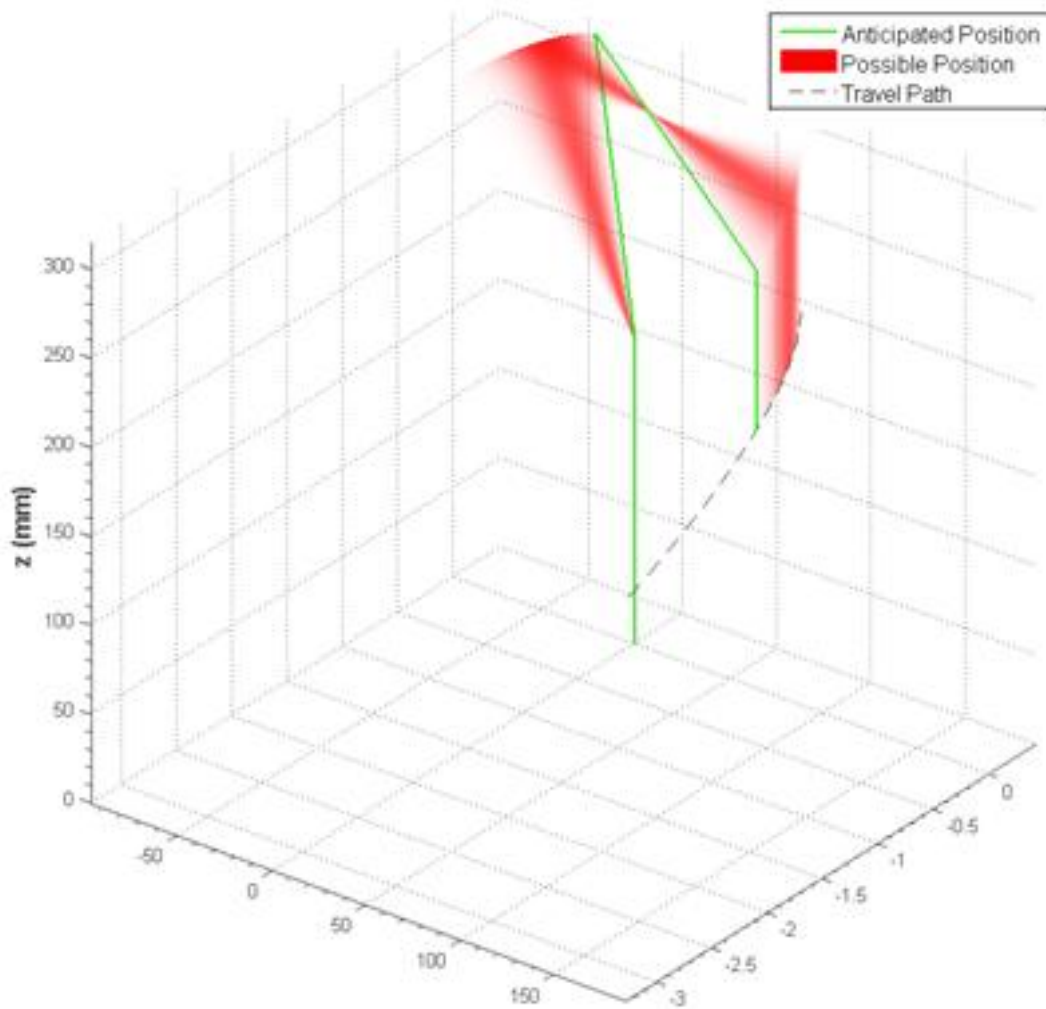
Figure 25 – Collision location estimation using IMU feedback

The collision estimation method described in this simulation can be installed in the laboratory robotic arm system. By doing so, the system could provide additional information to alert operators of where the collision has occurred. The information can also be used to limit future movement of the robot arm to avoid the collision area until operators have removed objects from the working area.

7. Summary

7.1 Conclusion

Improvements to infectious disease management is an ongoing challenge in order to respond to the increasing rates of infectious disease outbreaks. Biochemical processes, primarily those that are related to addressing disease diagnostics and surveillance, require robust solutions to ensure treatments and actions are made in a timely fashion. This can be facilitated through use of robust systems at each stage of infectious disease management, including automation systems to collect and analyse samples in laboratories, as well as stabilisation and simulation systems that improve field processes at an affordable cost.

In chapter 4, the importance of sample collection has been discussed as a vital stage of infectious disease management to effectively diagnose disease and plan treatment. The dried blood spot method for collecting blood samples is often used as it does not require needles like standard alternatives. If there is relative movement between the blood source and collection paper, the sample is often smeared which results in difficulties when analysed.

To replicate this issue, a simple rocking platform was developed to produce continuous motion between the blood source and collection paper. By attaching collection papers to gyroscopic stabilisers, the samples were shown to be collected more accurately. Results from analysis of blood impression distributions from numerous samples demonstrated the consistent reductions in spread of samples when stabilisers are used. The stabilisation systems have been demonstrated to effectively improve accuracy and consistency of blood sample collection.

In chapter 5, motion simulation platforms have been demonstrated as an effective tool to replicate motion characteristics of specimen transport systems by land or air. A low-cost simulation platform was developed using a Stewart Platform constructed from 6 inexpensive servomotors connected to simulation software via a microcontroller board. Real motion data collected from land-based vehicles in the field was accurately replicated by the platform for large motion fluctuations, however minor fluctuations were replicated with less precision due to issues with noise and servomotor limitations.

Large fluctuations in motion are factors for deterioration of biochemical samples due to effects from sloshing. Testing of simulated motion on samples of unpasteurised milk showed small reductions in pH levels, indicating a reduction in quality of the samples. These tests were conducted in a controlled lab in a cost-effective manner, which would otherwise require in field testing at the expense of cost and environment factors.

The benefits of simulation are further considerable for unmanned aerial vehicles where field tests are often limited by licence costs and environmental conditions. The platform simulator described in this study has been used to simulate motion of aerial vehicles in the field. The work described in chapter 6 extends this through the development of a low-cost gust simulator to measure the effects of gusts on various unmanned aerial vehicles without necessity of field collection. The system has demonstrated the ability to accurately replicate gusts at varying wind speeds, using a controlled wind tunnel without need for expensive tools or modification. The applications of these tools have been identified for UAV transportation of biochemical samples and aspects of UAV surveying as a tool for disease surveillance and prevention.

Once samples are delivered to the biochemical laboratory, automation-assisted processes ensure samples are analysed efficiently to plan treatment. Existing automation tools are often expensive or lack precision in some processes which leads to efficiency losses when samples are damaged or spilled. In chapter 7, a low-cost robot arm mechanism has been explored in this study as an affordable automation tool to process samples. A program was developed to allow the robot arm to move in smooth movements, and was demonstrated to pick up and move microplates. Inexpensive inertial sensors were interfaced with the robot arm to improve precision and develop feedback capabilities for collision detection. Any collisions or stalls in automated-processes result in delays requiring user remediation. A simulation was developed to demonstrate the ability of the robot arm to detect locations of collisions in order to efficiency alert operators of obstacles and continue operation by navigating around the known obstacle's location. This system demonstrates robust improvements to operation of automation processes in biochemical laboratories, ensuring low-cost mechanisms operate reliably and efficiently.

In summary, various biochemical processes outlined in this study have demonstrated improvements to reliability, efficiency and affordability compared to conventional methods. Low-cost tools developed offer direct benefits to laboratory and field processes, whilst simulation systems show promise for further exploration of innovative improvements to infectious disease management tools.

7.2 Recommendations

The following recommendations are made for improvements to biochemical processes in practice.

Robust processes identified in this study offer improvements to areas particularly where affordability is a limiting factor. Low-cost robot arm and stabilisation mechanisms are shown to improve efficiency and accuracy over conventional processes. Furthermore, improvements such as obstacle detection should be considered to ensure low-cost processes operate reliably.

The following recommendations are offered for related research to improvements in biochemical field and laboratory processes.

Simulation systems developed in this study provide affordable and reliable methods for testing and developing innovative transport systems. New technologies in this area can be tested using simulation to understand impacts of motion on samples in a controlled environment. Low-cost technologies demonstrated should be considered when determining appropriate simulation required. Inexpensive mechanisms like servomotors face limitations as simulation tools, and more precise systems may produce better results for situations where high degrees of accuracy is necessary such as vibration testing. Similarly, gust simulators can be used to test various UAV technologies to determine suitability for biochemical transportation in the field without requiring comprehensive field testing.

8. References

[1] K. F. Smith, M. Goldberg, S. Rosenthal, L. Carlson, J. Chen, C. Chen and S. Ramachandran, "Global rise in human infectious disease outbreaks," *The Royal Society,* vol. 11, no. 101, 2014.

[2] N. A. Christakis and J. H. Fowler, "Social Network Sensors for Early Detection of Contagious Outbreaks," *PLOS ONE,* 2010.

[3] K. M. Fornace, C. J. Drakeley, T. William, F. Espino and J. Cox, "Mapping infectious disease landscapes: unmanned aerial vehicles and epidemiology," *Trends in Parasitology,* vol. 30, no. 11, 2014.

[4] R. Felder, "Advances in Clinical Laboratory Automation," *AACC - Clinical Laboratory News,* 1 December 2014.

[5] M. C. Thurmond, "Conceptual foundations for infectious disease surveillance," *J Vet Diagn Invest,* vol. 15, pp. 501-514, 2003.

[6] *Deeks JJ. Systematic reviews in health care: Systematic reviews of evaluations of diagnostic and screening tests. Bmj. 2001;323(7305):157-62.*

[7] The Joanna Briggs Institute, "Joanna Briggs Institute Reviewers' Manual: 2015 edition / Supplement," The Joanna Briggs Institute, Adelaide, 2015.

[8] *White S, Schultz, T., Enuameh, YAK., ed. Synthesizing evidence of diagnostic accuracy. Philadelphia, USA: Lippincott Williams and Williams 2011.*

[9] C. W. Lam and E. Jacob, "Implementing a Laboratory Automation System: Experience of a Large Clinical Laboratory," *Journal of Laboratory Automation,* vol. 17, no. 1, pp. 16-23, 2012.

[10] The Lewin Group, "The Value of Diagnostics Innovation, Adoption and Diffusion into Health Care," AdvaMedDx, 2005.

[11] *G. Poste, Biospecimens, biomarkers and burgeoning data: the imperative for more rigorous research standards, Trends Mol. Med. 18 (2012) 717-722.*

[12] J. Zander, M. Bruegel, A. Kleinhempel, S. Becker, S. Petros, L. Kortz, J. Darow, J. Kratzsch, R. Baber, U. Ceglarek, J. Thiery and D. Teupser, *Effect of biobanking conditions on short-term stability of biomarkers in human serum and plasma, Clin. Chem. Lab. Med. 52 (2014) 629-639.*

[13] *R. Guthrie, A. Susi, A simple phenylalanine method for detecting phenylketonuria in large populations of newborn infants. Pediatrics 32 (1963) 338–343..*

[14] *L. Tretzel, A. Thomas, H. Geyer, G. Gmeiner, G. Forsdahl, V. Pop, W. Schänzer, M. Thevis, Use of dried blood spots in doping control analysis of anabolic steroid esters, J. Pharm. Biomed. Anal. 96 (2014) 21-30.*

[15] *S.F. Andriamandimby, J.-M. Heraud, L. Randrianasolo, J.T. Rafisandratantsoa, S. Andriamamonjy, V. Richard, Dried-blood spots: A cost-effective field method for the detection of Chikungunya virus circulation in remote areas, PLOS Negl. Trop. Dis. 7 (2013).*

[16] P. Smit, K. Sollis, S. Fiscus, N. Ford, M. Vitoria, S. Essajee, D. Barnett, B. Cheng, S. Crowe, T. Denny, A. Landay, W. Stevens, V. Habiyambere, J. Perriens and R. Peeling, *Systematic review of the use of dried blood spots for monitoring HIV viral load and for early infant diagnosis, PLoS One 9 (2014) e86461.*

[17] *Y. Bu, H. Huang, G. Zhou, Direct polymerase chain reaction (PCR) from human whole blood and filter-paper-dried blood by using a PCR buffer with a higher pH, Anal. Biochem. 375 (2008) 370-372.*

[18] *T. Ramesh, P. Nageswara Rao, R. Nageswara Rao, K.V.V. Satyanarayana, Hydrophilic interaction liquid chromatography for the determination of vesnarinone on dried blood spots; application to pharmacokinetics in rats, New J. Chem. 37 (2013) 3092-3099..*

[19] *T.J. Sullivan, M.S. Antonio-Gaddy, A. Richardson-Moore, L.M. Styer, D. Bigelow-Saulsbery, M.M. Parker, Expansion of HIV screening to non-clinical venues is aided by the use of dried blood spots for Western blot confirmation, J. Clin. Virol. 58 (2013).*

[20] J. Déglon, A. Thomas, Y. Daalib, E. Lauer, C. Samer, J. Desmeules, P. Dayer, P. Mangin and

C. Staub, *Automated system for on-line desorption of dried blood spots applied to LC/MS/MS pharmacokinetic study of flurbiprofen and its metabolite. J. Pharma. Biomed. Anal. 54 (2011) 359–367..*

[21] *N.J. Martin, J. Bunch, H.J. Cooper, Dried blood spot proteomics: Surface extraction of endogenous proteins coupled with automated sample preparation and mass spectrometry analysis, J. Am. Soc. Mass Spectrom. 24 (2013) 1242–1249..*

[22] *J.E.C. Burnett, Dried blood spot sampling: practical considerations and recommendation for use with preclinical studies, Bioanalysis 3 (2011) 1099-1107..*

[23] *M. Congedo, A. Lécuyer, The influence of spatial delocation on perceptual integration of vision and touch, Presence 15 (2006) 353–357..*

[24] *Felder RA. Preanalytical errors introduced by sample-transportation systems: A means to assess them. Clin Chem 2011;57:1349–50..*

[25] *Rosetti MD, Kumar A, Felder RA. Simulation of robotic courier deliveries in hospital distribution services. Health Care Man Science 2000;3:201–13.*

[26] *Dark Daily. http://www.darkdaily.com/researchers-at-livermore-national-laboratory-develop-microbial-detection-array-capable-of-detecting-thousands-of-known-and-unknown-pathogens-in-a-single-rapid-test#axzz3HTavrFO5 (Accessed October 28, 2014).*

[27] *Estey CA, Felder RA. Clinical trials of a novel centrifugation technique: Axial separation. Clin Chem 1996;42:402–9.*

[28] L. D. V. S. R. e. a. Gildea JJ, "A linear relationship between the ex-vivo sodium mediated expression of two sodium regulatory pathways as a surrogate marker of salt sensitivity of blood pressure in exfoliated human renal proximal tubule cells: The virtual renal biopsy," *Clin Chim Acta,* no. 421, pp. 236-242, 2013.

[29] *H. N. Abramson, Technical Report No. SP-106, NASA, 1967 (unpublished).*

[30] *M. W. Whittle, Human Movement Sc. 16, 347 (1997).*

[31] *G. A. Cavagna and P. Franzetti, J. Physiol. 373, 235 (1986)..*

[32] *G . A. Cavagna and R. Margaria, J. Appl. Physiol. 21, 271 (1966)..*

[33] *T. Öberg, A. Karsznia, and K. Öberg, J. Rehabil. Res. Dev. 30, 210 (1993)..*

[34] J. B. 3. 8. (. R. C. Wagenaar and R. E. A. van Emmerik.

[35] *J. M. Hausdorff, Y. Ashkenazy, C.-K. Peng, P. C. Ivanov, H. E. Stanley, and A. L. Goldberger, Physica A 302, 138 (2001)..*

[36] *F. T. Dodge, Technical Report (No. SP-106 updated), Southwest Research Institute, 2000 [http://snap.lbl.gov/pub/bscw.cgi/d87835/SwRI_SLOSH_Update.pdf]..*

[37] *A. Herczyński and P. D. Weidman, J. Fluid Mech. 693, 216 (2012)..*

[38] *R. A. Ibrahim, Liquid sloshing dynamics: Theory and applications (Cambridge University Press, Cambridge, 2005)..*

[39] *H. N. Abramson, Technical Report No. SP-8031, NASA, 1969 (unpublished)..*

[40] *C. G. Langner, Technical Report No. 7, Southwest Research Institute, 1963 (unpublished)..*

[41] H. C. Mayer and R. Krechetnikov, "Walking with coffee: Why does it spill?," *Physical Review E,* vol. 85, no. 4, 2012.

[42] R. L. Smith, "Predicting Evaporation Rates and Times for Spills," *The Annals of Occupational Hygiene,* vol. 45, no. 6, pp. 437-445, 2001.

[43] M. E. Moran, "Evolution of robotic arms," *Journal of Robotic Surgery,* vol. 1, no. 2, pp. 103-111, 2007.

[44] A. Sparkes, W. Aubrey, E. Byrne, A. Clare, M. N. Khan, M. Liakata, M. Markham, J. Rowland, L. N. Soldatova, K. E. Whelan, M. Young and R. D. King, "Towards Robot Scientists for autonomous scientific discovery," *Automated Experimentation,* vol. 2, no. 1, 2010.

[45] Nair and P. P., "Robot arm and method of controlling robot arm to avoid collisions". California, United States of America Patent 8,340,820, 26 February 2010.

[46] N. Ahmad, R. A. R. Ghazilla, N. M. Khairi and V. Kasi, "Reviews on Various Inertial Measurement Unit (IMU) Sensor Applications," *IJSPS,* vol. 1, no. 2, 2013.

[47] S. Won, F. Golnaraghi and W. Melek, "A fastening tool tracking system using an IMU and a position sensor with Kalman filters and a fuzzy expert system," *IEEE Trans. Ind. Electron.,* vol. 56, no. 5, pp. 1782-1792, 2009.

[48] S. h. P. Won, "A fastened bolt tracking system for a handheld tool using an internial measurement unit and a triaxial magnetometer," *Proc. 35th Annual Conf. of IEEE Industrial Electronics,* pp. 2703-2708, 2009.

[49] K. King and e. al, "Bowling ball dynamics revealed by miniature wireless MEMS inertial measurement unit," *Sports Eng.,* vol. 13, no. 2, pp. 95-104, 2011.

[50] T. S. Bruggemann, D. G. Greer and R. A. Walker, "GPS Fault detection with IMU and aircraft dynamics," *IEEE Trans. Aerospace and Electronic Systems,* vol. 47, no. 1, pp. 305-316, 2011.

[51] W. W. Wang and L. C. Fu, "Mirror therapy with an exoskeleton upper-limb robot based on IMU measurement system," in *IEEE International Workshop on Medical Measurements and Applications Proceedings (MeMeA)*, 2011.

[52] M. Hutter and e. al, "Starleth: A compliant quadrupedal robot for fast, efficient, and versatile locomotion," *Proc. Int. Conf. Climbing and Walking Robots,* 2012.

[53] L. Nehaoua, E. V. d'Essonne, R. d. Pelvoux, H. Arioui and S. Mammar, "Review on single track vehicle and motorcycle simulators," in *Control & Automation (MED), 2011 19th Mediterranean Conference*, Corfu, Greece, 2011.

[54] *T. Rosnell, E. Honkavaara, Point cloud generation from aerial image data acquired by a quadrocopter type micro unmanned aerial vehicle and a digital still camera, Sensors (Basel) 12 (2012) 453–480..*

[55] *G. Wu, J. Srivastava, M.H. Zaman, Stability measurements of antibodies stored on paper, Anal. Biochem. 449 (2014) 147-154..*

[56] *D. McMorran, D.C.K. Chung, J Li, M. Muradoglu, O.W. Liew, T.W. Ng, Adapting a low-cost selective compliant articulated robotic arm for spillage avoidance. J. Lab. Automation. DOI: 10.1177/2211068216630742..*

[57] *E.R. Wickremsinhe, E.J. Perkins, Using dried blood spot sampling to improve data quality and reduce animal use in mouse pharmacokinetic studies. J. Am. Assoc. Lab. Anim. Sci. 54 (2015) 139-144..*

[58] M. F. McCabe, R. houborg and J. Rosas, "The potential of unmanned aerial vehicles for providing," in *21st International Congress on Modelling and Simulation*, Gold Coast, Australia, 2015.

[59] B. Mendelow, P. Muir, B. T. Boshielo and J. Robertson, "Development of e-Juba, a preliminary proof of concept unmanned aerial vehicle designed to facilitate the transportation of microbiological test samples from remote rural clinics to National Health Laboratory Service laboratories.," *SAMJ,* vol. 97, no. 11, pp. 1215-1218, 2007.

[60] D. L. K.-R. C. S.-Y. J. J.-H. K. C.-O. M. D.-I. H. S.-J. C. J.-H. Kim, "Development of an electro-optical system for small UAV," *Aerosp. Sci. Technol.,* vol. 14, pp. 505-511, 2010.

[61] P. C. F. T. P. Sandoval, "Evaluating the longitudinal stability of an UAV using a CFD-6DOF model," *Aerosp. Sci. Technol,* vol. 43 , pp. 463-470, 2015.

[62] R. S. M. S. A. B. K. M. U. A.-S. S.U. Ali, "Lateral guidance and control of UAVs using second-order sliding modes," *Aerosp. Sci. Technol.,* vol. 49, pp. 88-100, 2016.

[63] S. M. A. T. Y. Inoue, "A blimp-based remote sensing system for low-altitude monitoring of plant variables: A preliminary experiment for agricultural and ecological applications," *Int. J. Rem. Sens. ,* vol. 21, pp. 379-385, 2000.

[64] P. N. N. K. N. P. D. M. C. K. N. F. R. L. A. D. W. K. J.A. Shaw, "Multispectral imaging systems on tethered balloons for optical remote sensing education and research," *J. Appl. Rem. Sens. 6,* 2012.

[65] D. Buell, "An experimental investigation of the velocity fluctuations behind oscillating vanes," *Technical Note D-5543, NASA, Ames Research Center, Moffett Field, CA,* 1969.

[66] J. B. A. Parker, "A wind-tunnel stream oscillating apparatus," *J Aircraft,* vol. 9, p. 446–447, 1972.

[67] P. C. E. D. D.M. Tang, "Experiments and analysis for a gust generator in a wind tunnel," *J Aircraft,* vol. 33, p. 139–148, 1996.

[68] M. C. A. M. S. Zarovy, "Experimental method for studying gust effects on micro rotorcraft," *Proc IMechE G: J Aerosp Engin,* vol. 227 , p. 703–713, 2012.

[69] *T.W. Ng, A. Tajuddin, Shadow moire topography using a flatbed scanner. Opt. Engin. 41 (2002) 1908-1911..*

[70] *T.W. Ng, P K Quek and K H Lim, Phase shifting photoelasticity using a flatbed scanner. Opt. Engin. 42 (2003) 2375-2379..*

[71] J. J. S. Chandrapala, *Effect of Concentration, pH and Added Chelating Agents on the Colloidal Properties of Heated Reconstitued Skim Milk,* 2008.

[72] *Denavit, J.; Hartenberg, R.S. A kinematic notation for lower-pair mechanisms based on matrices, Trans. ASME J. Appl. Mech. 1955, 23. 215–221..*

[73] D. Prohasky and S. Watkins, "Low Cost Hot-element Anemometry Verses the TFI Cobra," in *19th Australasian Fluid Mechanics Conference*, Melbourne, 2014.

[74] J. B. A. Parker, "A wind-tunnel stream oscillating apparatus," *J Aircraft,* vol. 9, p. 446–447, 1972.